Alma Mater Studiorum – Università di Bologna

DOTTORATO DI RICERCA IN

SCIENZE E TECNOLOGIE AGRARIE, AMBIENTALI E ALIMENTARI

Ciclo 35

Settore Concorsuale: 07/C1 INGEGNERIA AGRARIA, FORESTALE E DEI BIOSISTEMI

Settore Scientifico Disciplinare: AGR/09 MECCANICA AGRARIA

AN APPROACH TO DIGITALISE ACTIVITIES OF COMBINE HARVESTERS THROUGH CANBUS

Presentata da: Dott. Enrico Michielan

Coordinatore Dottorato

Prof. Massimiliano Petracci

Supervisore

Prof. Ing. Michele Mattetti

Co-Supervisore

Prof. Maurizio Canavari

Esame finale anno 2023

An approach to digitalise activities of combine harvesters through CANBUS

Dott. Michielan Enrico

Abstract

The increase in the efficiency of agricultural machinery is a theme that attracted the attention and investments of the industrial and research community. In addition, in a global market, where the prices of agricultural commodities are so volatile and the prices of the inputs increase, farmers and agricultural contractors struggle to obtain at the end of the agricultural season a consolidated profit. For these reasons, it is important to carefully plan the usage of combine harvesters, to reduce the unproductive time and the input usage such as the fuel, that at the end of the harvesting season could increase costs.

This study aims to develop an algorithm able to automatically identify and evaluate the time spent by the combines in each of the identified activities, identify the field boundaries of the harvested fields and perform a performance evaluation. To be able to develop the algorithm, during the harvesting seasons of 2020 and 2022, two combine harvesters operating in real-world conditions in Bologna's Province were monitored. The data necessary to perform the analysis were acquired as CANBUS data and processed by using the MATLAB ® suite.

The results obtained from this analysis show that the monitored combines have spent over 60% of the time performing harvesting activities, 13% of the time idling at the field, 10% performing headland turn, the 3% and 4% of the time respectively in transport on the field and road and 2% of the time in unloading. In addition, the performance of the monitored combines resulted similarly to the performance reported in other studies.

“The first rule of any technology used in a business is that automation applied to an efficient operation will magnify the efficiency. The second is that automation applied to an inefficient operation will magnify the inefficiency”.

Bill Gates

Declaration

I hereby declare that the following thesis is the result of my PhD research carried out over three years. Contributions from other authors have been appropriately cited and reported in the bibliography. This thesis is original and has not been submitted to any other institution or university for the achievement of other qualifications or degrees.

Enrico Michielan

Bologna, December 2022

Acknowledgements

Before finishing the Ph.D., I want to take few lines to thank some key people without whom this work was not possible:

To all my family and to my girlfriend for their support and understanding during these years.

Professors Giovanni Molari and Michele Mattetti for making me passionate about the agricultural engineering and mechanics, and to give me the chance and the privilege to work together.

Professor Claus Sørensen for having opened the doors of his institute and for having shared his passion and his deep knowledge about smart agriculture.

My old and new office mates, Nicolò Regazzi, Francesco Motti, Leonardo Angelucci, Gianvito Annesi and Luca Colendi for moments of hilarity, pleasant work and knowledge-sharing spent together.

1 Contents

List of Figures

List of Tables

List of Symbols

Symbol	Description	Unit of measure
NIR	Near Infrared Reflectance	-
GNSS	Global Navigation Satellite System	-
GHG	Greenhouse Gasses	-
ECU	Electronic Control Unit	-
SD	Secure Digital	-
CANBUS	Control Area Network	-
GIS	Geographic Information System	-
PA	Precision Agriculture	-
FMIS	Farm Management Information System	-
HED	Holistically-Nested Edge Detection	-
LPIS	Land Parcel Identification System	-
EC	European Communities	-
CAP	Common Agricultural Policies	-
DL	Deep Learning	-
SIGPAC	Geographical Information System for Agricultural Parcel	-
MD-FCN	Multiple Dilation Fully Convolutional Network	-
SCR-Net	Super Resolution Semantic Contour Detection Network	-
BRP	Basic Registration Crop Parcel	-
AFB	Agricultural Field Boundaries	-
DBSCAN	Density Based Spatial Clustering of Application with Noise	-
OD	Object Detection	-
CEP	Circular Error Probable	-
4WD	Four Wheel Drive	-
MFWD	Mechanical Front Wheel Drive	-
DP	Dwell Period	-
PTO	Power Take Off	kW
TFR	Threshold Fuel Rate	L h^{-1}
NAS	Network Attached Storage	-
T_{er}	Engine Reference Torque	N m^{-1}
T_{ae}	Actual Engine Percent Torque	-
T_{nf}	Nominal Friction-Percent Torque	-
n_e	Engine Speed	rad s^{-1}
$\dot{F}_r$	Engine Fuel Rate	L h^{-1}
H_{dd}	Header Down	-
$\dot{C}_f$	Crop Flow	g s^{-1}
U_{EA}	Unload Engine Auger	-
V	Navigation Based Vehicle Speed	km h^{-1}
α_{CB}	Compass Bearing	deg
x_a	Polar coordinates of the point a of the header	m
y_a	Polar coordinates of the point a of the header	m
x_b	Polar coordinates of the point a of the header	m
y_b	Polar coordinates of the point a of the header	m
H_w	Header width	m
P_{eng}	Power engine	kW
C_{Yield}	Crop yield	t ha^{-1}
F_{cons}	Fuel consumption	L
F_{sr}	Field shape ratio	-

t	Duration	s
F_c	Field capacity	ha h^{-1}
C_{YHi}	Crop yield per each field	t ha^{-1}
F_{consHi}	Fuel consumption per each field	L
$\bar{P}_{engi}$	Mean power engine measured in each field	kW
$\bar{V}_i$	Mean speed measured in each field	km h^{-1}
A	Area of the harvested field	ha
P	Perimeter of the harvested field	m

Chapter 1

1. Introduction

1.1 Problem description

Farmers and agricultural managers struggle to obtain a profit at the end of the harvesting season, and this pushed researchers to investigate the performance of every single activity carried out for growing crops. This is necessary in order to cut the operational costs of machines which are accounted for almost 30%[1].

The performance of agricultural machinery increased thanks to technological developments which led to an increased in the size of agricultural machinery, a reduction in the required workforce, and an increase in machinery's functionalities. All these improvements permitted to increase field capacities, grain quality, and minimise losses. Field capacity is the area covered by agricultural machinery in an hour and it represents a key parameter for performance evaluation. Instead, grains quality ensembles several characteristics such as physical (i.e., moisture content, bulk density, etc.), safety (i.e., absence of fungal infections, mycotoxins, etc.), and compositional factors (i.e., protein content, starch content, etc.).

Researchers investigated a wide range of agricultural activities, in order to find possible inefficiencies and provide possible solutions to increase the field capacity. Most of these investigations are related to tillage and crop protection activities and only a few have investigated harvesting activities. However, most of these analyses were performed in constrained conditions which do not completely represent what happens in real working environment because if operators know that they are involved into a research activity, they may change their behaviour influencing the results. In this thesis, the activities carried out by combine harvesters operating in real-world conditions were monitored during an entire harvesting season, in order to investigate in which and how combine harvesters are effectively used on fields. In particular, this thesis reports a methodology to:

- Classification of the operational states;
- Classification of fields and estimation of the field boundaries;
- Estimation of the parameters that permit to evaluate combine performance and their comparison with the data reported in the literature.

1.2 Technological development in combine harvester and profit reduction in agricultural companies

Since the development of the first combine, pulled by horses, equipped with a steam engine and requiring at least four operators, many technological developments had been made [2]. The first and most important development was mounting a combustion engine making them self-propelled; thus, they could simultaneously move and process crops. This improvement was achieved during a crucial historical moment, the Second Industrial Revolution (between XIX and XX century), in which industry become a leading sector in most developed economies. This growth of industry resulted in an increase in the industry's workers' salaries that attracted people from rural areas to the cities, with a consequent workforce reduction in agriculture. Indeed, as reported by Federico and Malanima, in Italy as well as in most of the developed countries, since the end of the XX century the amount of agricultural workforce was reduced to 5% of the total [3]. In addition, for almost thirty years since the end of the Second Industrial Revolution, the world faced two world wars that created a reduction in food availability; however, at the end of this period, the world population grew rapidly as well as the food's request. To support these two demands, agricultural manufacturers developed new agricultural machinery and implements, where the demanded workforce was reduced and at the same time field capacities and grains quality increased. In combine harvesters, the cutter bar width was increased together with the size of combines, engine thrust and tank capacity. This led to more powerful and heavier machines able to process a greater amount of grain. Then, combines were equipped with electrically controlled systems and this allowed engineers to access a wide range of information that furtherly increased the efficiency of combine harvesters. The electronics simplified the work of the operator and opened the possibility of mounting different kinds of sensors like moisture meters, and near-infrared spectrometers (NIRs) and permitting to obtain real-time information about the combine's performance, settings and grain quality.

The application in agriculture of global navigation satellite systems (GNSSs) permitted to obtain the global position of a vehicle from a constellation of satellites and introduced the possibility of geo-referencing the beforementioned data and the development of automatic guidance systems [4]. In particular, the combination of information coming from yield monitors and GNSS receivers permitted to monitor the variability of crop yield in a field helping farmers in their site-specific crop management [5]. The aforementioned technological development in combine harvesters had, as a consequence, increased the purchase and service prices of these complex agricultural machinery [6]. Indeed, as reported by Mimra and Kavka [7], the purchasing price of combines increased by 24% from 2008-

2015. But in modern combines, not only the purchasing price has been increased but also the repair and maintenance costs. Indeed, in modern combine harvesters, many components could fatally increase the probability of malfunctions or failures and can cause an increase of repair and maintenance costs. Indeed, as stated by Calcante et al. [8], the repair and maintenance costs generally represent 10 ÷ 15% of the total costs of combines, but these costs could increase with the age of the machinery. These cost items, together with fuel cost, represent, in economic terms, a variable cost and they change with the increase of the annual use. Other budget items that must be considered are the commodities prices, which belong to the cereal price and the fuel price. Indeed, the cereal price represents a source of revenue for farmers and agricultural managers, and a variation of this budget item can influence the profit; while the fuel price represents an expense item and can consequently increase the costs. These price variation of the commodities are related to a worldwide phenomenon known as globalisation. The globalisation of commodity's market introduced the concept of uncertainty, because the pricing is no longer dependent to national factors but instead to global factors and those prices normally present monthly market fluctuations. Nowadays, farmers and agricultural managers struggle to make a profit at the end of the harvesting season due to the change of the above-mentioned budged items. This means that farmers and agricultural managers must reduce the costs. This goal can be achieved by increasing the annual utilization of the combine harvesters as reported by Mimra and Kavka in their study [7]. Moreover, nowadays technological development is not able to furtherly increase the efficiency of combines, due to tight international standards about the reduction of the emission of greenhouse gasses (GHGs) [9] and problems with soil compaction [10,11]. For these reasons, researchers started to investigate other possible ways to increase the combine's efficiency and consequently the profit. Some researchers started to monitor the fleet focusing on the importance to optimise machinery size [12]. Specifically, the optimal machinery size is dependent on interactions between machinery and the biological and meteorological systems [12]. From those analyses, it was discovered that to increase productivity and reduce the costs of agricultural machinery, it is mandatory to plan and control the use of resources in arable farming. This is true, especially for large machinery, such as combine harvesters, in which it is important to maintain a high efficiency by limiting non-productive times which represents a higher proportional loss in potential machine production [13]. To reduce the amount of time spent on non-productive activities and increase efficiency is necessary to increase the management and planning capability of farmers and agricultural managers, this is possible thanks to fleet management tools. These instruments, developed for the transport business, have found an application also in

agriculture, to increase scheduling activities, operational efficiency and effectiveness [14]. Other researchers monitored how the operator's skill can influence harvesting performance [15], while others monitored the machinery in it is entirety [16]. Each one of the proposed solutions can in a certain way increase the profit, but to provide to farmers and agricultural managers with the best solutions is mandatory to collect and store a wide range of information about the use of combine harvesters in real-world conditions.

1.3 Literature review

The possibility of a further increase efficiency of combine harvesters, and in general of agricultural machinery, attracted the attention of researchers since the advent of precise agriculture and international policies (2013-2020) about GHGs. In literature, there are many studies about different methodologies adopted for monitoring and analysing different farming activities. To obtain a complete picture of the harvesting activity performed by combines, it was decided to break this study down into three different steps:

1. Identify a way to acquire a wide range of data from agricultural machinery and classified it into tasks.
2. Identify the harvested field boundaries and obtain information about their parameters and characteristics.
3. Obtain and analyse the operational performance of the combine harvesters during harvesting season.

This choice was made because in this way it was possible to deeply understand each aspect of the harvesting activity and at the same time it permits to identify possible relations between each one of the three parts in which the activity was split.

1.3.1 Data acquisition and automated task identification

For accomplishing the before mentioned steps, data coming from real usages of combine harvesters must be properly collected. Thanks to technological development, nowadays this operation is easier to perform than in the past. Indeed, the development performed of a communication protocol called Control Area Network (CANBUS) by Bosch and it is adoption by agricultural machinery manufacturers [17] led many researchers to analyse CANBUS technologies [18,19]. CANBUS technology is based on a multiplex communication network where there are no master or slave devices in the system; indeed, the devices connected to the network can freely transmit messages, that contain information,

by using a unique message identifier (IDs). In the CANBUS network, communication occurs between the electronic control units (ECUs) displaced in different parts of the machinery as shown in Figure 1.1. The ECUs are microcontrollers that monitor, control and/or interface with some function of machines. The CANBUS network presents standard CAN messages but manufacturers can create proprietary CAN messages, to improve machinery management and performance by including more sensors [20].

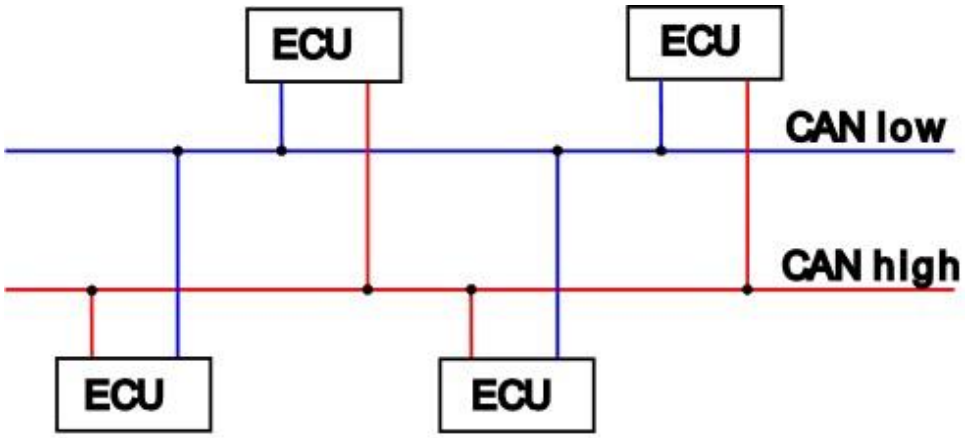

Figure 1.1: Electric scheme of the CANBUS network

The combination of CANBUS and GNSS receiver provided researchers with a wide range of information and opened the possibility to analyse and understand how agricultural machinery were used in their daily tasks without installing bulky and expensive sensors where their durability in field conditions cannot be guaranteed.

In order to be able to identify the best methodology to acquire a wide range of data and to identify the tasks in which the combines are involved during harvesting season, several research about data acquisition and/or tasks analysis were investigated. For these reasons, the investigated studies are not referred exclusively to combine harvesters but also to other kinds of agricultural machines which embed CANBUS technology, such as agricultural tractors. Böttinger and Fliege monitored seven Claas Lexion 580 combines with a data logger for evaluating the working performance of cleaning units of combine harvesters on sloped fields and recorded operational parameters such as the ground speed, the inclination of the machine, the position, machine adjustments, grain loss and throughput [16]. The authors explained that the obtained data sets were checked for validity and uncertain data set were filtered out. From the analysis of these parameters, the authors were able to understand how the cleaning unit worked on hillside terrains. The proposed methodology showed how to automatically acquire a large amount of data from combine harvesters, but in this study, there was not reported any information related to the data logger chosen or the approach

used for the data analysis, and the authors considered only the evaluation of the cleaning system. Instead, Molari et al. in their research used a data logger developed by Vector Informatik GmbH, Stuttgart, DE (i.e., CANcaseXL log) where data were stored on a secure digital (SD) card. In this study, they monitored for an hour a tractor in three different tasks such as trailer transportation, cultivation and ploughing. The research aimed to identify which was the most used gear in each operation [18]. The proposed methodology showed a possible solution to record different signals from the CANBUS network about tractor usage. In a study performed by Salim et al., a John Deere 9430 was monitored to evaluate its performance through CANBUS data. The analysis was performed in a field that was divided into three blocks of 16 strips each, and CANBUS data were collected with a laptop connected to a CANBUS analyser developed by Vector (i.e., VN 1610). In this case, it was also created a backup data set by using a Vector GL1000 data logger and data were statistically analysed through SAS software (SAS Institute Inc., Cary, North Carolina 27513, USA). In this analysis, the researchers monitored the fuel rate, position, slip percentage and effective field capacity, the first two information were obtained by the CANBUS while the field capacity was indirectly obtained. But regarding the device's configuration, the proposed one results are too complex [21]. In all the before mentioned studies, the operator had to turn on and off the data recording process limiting the amount of recordable data and therefore the generalizations of the research results. Indeed, collecting data in the most realistic conditions is crucial to make the operator unaware of the recording process [22]. Molari et al. were the first to extensively record CANBUS data in the most realistic conditions and they adopted a stand-alone CANBUS data logger optimised by CNH Industrial and a dash-camera [23]. The data logger was able to automatically record all the CANBUS messages every time the tractor engine was turned on, while the camera recorded what happened during idle. The data analysis was carried out with MATLAB (MathWorks Inc., Natick, MA, USA) and to individuate the idling conditions they developed an algorithm that create a logical variable that was set to 1 anytime the tractor was in a standing position and the PTO was not engaged while was 0 otherwise. Even if this study helped to design an extensive data collection of CANBUS data, the analysis was mostly focused on the analysis of a specific operating state of the tractor (i.e., idling). The adoption of a camera that recorded what happened every time the vehicle was in idle condition could be a prosecution of the efficiency analysis in combine harvesters. Mattetti et al. in their analysis, proposed a solution to outline the mission profile of agricultural tractors by using CANBUS data analysis [19]. In this study, the data were acquired by using the same device adopted by Molari et al. [23], that has allowed to acquire the data for almost 107 days. While the data analysis was performed by using MATLAB and

an ad hoc algorithm that was able to identify all the operating activities, in which tractors are typically involved. The methodology proposed by Mattetti et al. presents all the characteristics required to perform an automated identification of the tasks in which combines were involved during harvesting season both for the chosen data logger and for the algorithm presented for the data analysis.

1.3.2 Automated field boundaries identification

As reported by Webster and Oliver, the earth's surface is heterogeneous, but it could change multiple times and create a sort of endless variety [24]. The point of view of these two researchers perfectly explains the concept at the basis of precision agriculture (PA) in which the parameters could change in space and time. The application of PA would have not been possible without the development of certain technologies such as computers, GNSS, geographic information systems (GIS), sensors and application control [25].

Each year, the land cover and the boundaries of the field could changes accordingly with the planned crop rotation or due to the shifts in agricultural markets and policy initiatives [26]. So, if farmers or agricultural managers want to have access to agricultural funds or want to develop a historical database where stores all information about the monitored parameters for each field, the delineation of field boundaries is an operation that farmers and agricultural managers have to perform every year. In the early fleet management solutions developed by agricultural machinery manufacturers, the field boundary delineation had to be performed by the operator with a tractor equipped with a GNSS receiver. This operation was carried out by setting on the monitor the recording mode and running the tractor around the field boundaries. At the end of the process, the operator had to stop the acquisition, set a field name, and save the acquired information. This procedure is mandatory for using automatic guidance systems and it must be carried out any time there is a change in field boundaries. This leads to an unproductive use of tractors in a cropping cycle. Thanks to software developers and researchers, this operation is nowadays easier since it can be carried out with Farm Management Information Systems (FMISs) using satellite maps. Even if this avoids the unproductive use of machinery, the operation nowadays remains manual.

For these reasons, researchers began to look for more efficient and less time-consuming solutions to automate the identification of field boundaries. The solutions found in literature can be divided into two groups in function of the data source used: based on the satellite images and on machinery trajectory measured with GNSS receivers.

By starting from the solutions that permit the use of satellite imagery or that come from unmanned aerial vehicles, one of the proposed ideas was based on the use of a multi-stage

approach for segmenting field objects. This approach, proposed by Marvaniya et al, was developed with the purpose to automatically identify the field boundaries of small fields which was not investigated before. The authors identified croplands by adopting a reversed method, in which were excluded non-agricultural lands (forests, villages, grassland) [27]. This goal was achieved by applying to the acquired aerial imagery the global land cover mask provided by Buchhorn et al. [28]. After this first stage, contour detection was performed, only on the regions identified as croplands, by applying the Holistically-Nested Edge Detection (HED) technique. This technique consists in edge detection where, a sort of clean-up of the output data was performed by applying image operations such as erosion, dilation, and explicit edge thinning. This operation resulted mandatory because the algorithm can misclassify polygons, for the following reasons:

- Areas without crop fields or with small isolated buildings, built up or non-crops areas inside an area considered as croplands.
- Polygons can be formed by multiple fields.
- A single field can be split into multiple polygons and identified as multiple fields.

To reduce the risk of misclassification, the authors applied a methodology based on a heuristics method based on a deep knowledge of the field characteristics such as the convexity, size and aspect ratio. The authors meant aspect ratio a ratio between the average width and perimeter of the polygons. This correction of the data was performed by setting different threshold values related to:

- A minimum area and perimeter, in which all the fields with those parameters lower than a threshold value were excluded.
- A minimum value of convexity of the fields, where the fields excluded from the analysis do not have a ratio of the area of the convex hull drawn around the identified polygon to the area of the polygon itself were not too large.
- A minimum ratio between the area and the perimeter of the field, in which the fields that pass the previous two thresholds need to present a threshold ratio between area and perimeter.
- A minimum aspect ratio of the polygons, in which the identified polygons that have passed the previous three tests were excluded whenever the aspect ratios of the polygons were below the set threshold value.

Once obtained this first polygon's classification, the attention of the authors shifted to verify if the identified polygons were composed of a single polygon or by a group of polygons. To obtain this information, the authors checked the absence of the polygon's boundary of cut

points; Marvaniya et al considered as cut points all the lines along which large polygons can be split. In order to be able to identify the field boundaries in each situation, the authors at the end of the previous steps, performed on each identified polygons a second-level "localized" contour detection. To be able to perform this analysis the authors adopted the Canny edge detector methodology[29], in which were checked the pixels present in the image. This analysis was performed by applying a Gaussian filter to remove the noise, individuate the maximum intensity gradients for the image, and compare the gradient intensity with the gradient direction of each pixel in order to be able to identify if the pixel analysed is linked to the one that follows. If this relation is true, then those two pixels could be considered as edges. To reduce even more misclassification two threshold gradient values were set named as low and high threshold; thus, pixels were classified into three groups:

- Strong: any time the gradient value of the pixel is higher than the high threshold.
- Weak: any time the gradient value of the pixel is between the low and high thresholds.
- Suppressed: any time the gradient value of the pixel is lower than the low threshold.

In the end, to be sure to have recognised only agricultural fields and exclude residual portions of buildings or natural vegetation sited inside agricultural regions, the authors performed a training phase of the algorithm, in which they created a data set containing information about the spectral and shape features of agricultural and non-agricultural fields [27]. The solution proposed by Marvaniya et al. revealed that the adoption of a multi-stage approach helped to perform an automated field boundaries identification, and it could be performed also for small fields. In addition, deep learning approach normally requires a wide number of images (10,000 to 50,000) for the training phase, but in the proposed methodology this number can be reduced to 25. The methodology proposed by the authors can find an application in this analysis because it was able to identify both small and big field boundaries, the problem is only related to the required computing power by the proposed algorithm; for the above-mentioned reason, this approach could not be considered.

Garcia-Pedrero et al. proposed an approach based on deep learning [30]. In particular, they proposed the use of the Land Parcel Identification System (LPIS), a web portal developed for the European Community (EC), in which are reported all boundaries and areas of the parcel eligible for the payment of the Common Agricultural Policy (CAP). This portal, as reported by the authors, can provide a sort of cadastre of agricultural fields per each state member and the information within this platform are useful for studying and monitoring various aspect of agricultural activities [31]. This portal was usually kept updated in order

to reduce the risk of paying sanctions due to improper identification of agricultural lands. Authors stated that the updating procedure is laborious and prone to human error process [32] performed by photo-interpretation of high resolutions orthophotos [31]. In their analysis, Garcia-Pedrero et al. proposed a solution based on deep learning (DL) where 207 raster tiles provided by the SIGPAC were considered. As reported by the authors, the SIGPAC is the Spanish name for the LPIS; for each of the raster tiles, it was available also the boundaries of agricultural parcels, water bodies, and cities. From the available data, the authors selected only the parcels corresponding to the following land cover classification: fruit trees, nuts, olive groves, orchards, arable lands, and vineyards. The information provided by this selection were used by authors as ground truth; in which the ground truth represents a data set that can be used for the training phase of the deep learning algorithm. To be able to automatically identify agricultural boundaries, the authors applied a U-Net methodology, based on a convolutional neural network model where for the training phase, they used the information provided by the LPIS. As stated by Garcia-Pedrero et al, the application of this methodology presented a problem, which turns out to be related to the computational requirements to perform the training phase. For this reason, the authors reduced the spatial resolution of the data set to 1.173 by 1.173 pixels by using the nearest neighbour algorithm and applied the same resolution also to the rasterized ground truth data set. To perform a good training phase and avoid over-fitting, the data set had a high variability and for this reason, the authors adopted a random Dihedral transformation. As stated by the authors, the adoption of a deep learning methodology allowed a very good performance of field boundaries identification from different images. The proposed methodology could not be used to perform an automated field boundaries identification if the kind of data used by the authors were not easily available and if there is not a required computational capacity.

Another adopted solution consisted in the use of satellite images coming from the Sentinel-2 satellite. These images present a medium spatial resolution but are freely available, with an open data policy [33–35]. Sentinel-2 images are usually used for crop classification because the images present good spectral information and medium spatial resolution, these features make these imageries suitable for agricultural field boundaries identification. In this research, performed by Masoud et al. [36], it was developed a multiple dilation fully convolutional network (MD-FCN) and a super-resolution semantic contour detection network (SCR-Net) to perform pixel-wise image analysis. As seen in other studies these deep-learning approaches were trained to extract semantic information from satellite images. In this analysis, the authors used Sentinel-2 and RapidEye images of Flevoland in The

Netherlands, and to perform the automated field boundaries identification, a basic registration crop parcel (BRP) dataset downloaded from a Dutch governmental open platform, that offers up-to-date geodata. As reported by the authors, the BRP dataset contains information about land use in the Netherlands and is divided into five attributes: arable land, grassland, wasteland, natural and other. Thanks to this dataset, Masoud et al. were able to define agricultural field (arable land and grassland), non-agricultural field (wasteland, natural and other) and agricultural field boundaries (AFB). For the authors, AFB was represented by the outer extent that defines the transition from one field to another or from a field to a non-agricultural field. At this point the authors identified, from the Sentinel-2 dataset, 10 tiles with the same size as ground truth for the training and for the testing, the same thing was performed for the RapidEye dataset. As mentioned by the authors, the analysis was performed previously only on two tiles, this part was necessary to set filter size, patch size and the training samples, after on the entire dataset. When the AFB were identified from the dataset, the authors performed an accuracy assessment by using an F-score. As reported by the authors, the proposed methodologies worked properly for automated field boundaries identification both at local and national scales. The only limitation is represented by the accuracy of the dataset used for the training phase. A negative aspect of this methodology is its computational demand; indeed, Masoud et al. report that the training phase for MD-FCN and SCR-Net model from a tile of 800 x 800 pixels with a 10 m resolution requires roughly 2 and 4 hours [36]. The proposed methodology is surely interesting but hardly can find an application in the analysis, due to the fact that it requires a great computational demand.

Another technique family is the identification of field boundaries using machinery trajectory when they operate on the field. The advantage of these technique families is that it does not require access to weather-dependent satellite imagery in the area and it requires a low computational capacity and a relatively low-cost instrumentation. These approaches permit obtaining information about the harvested fields in all weather conditions and all over the world as long as the machines work in an area and can be implemented easily on combine harvesters. Chen et al. [37] performed an analysis of a dataset acquired in China in 2019 aiming to identify fields and road segments. To perform this analysis, the authors cleaned the data in order to avoid the influence of signal noise that may occur during data acquisition. To reach this goal, incorrect GNSS points were detected by using the maximum speed reached by the vehicle [38]. To each of the remaining points, the authors applied the nearest neighbour smoothing method which replaced the GNSS coordinates with the mean value of the geographical coordinates of its closest points [39,40]. The authors have also performed

filtering of duplicate points because whenever the combine was in a standing position generated duplicate points that needed to be excluded from the dataset, otherwise the algorithm individuates abnormal points density during the clustering phase. After performing the data cleaning the authors carried out the DBSCAN clustering, in which the clusters were defined on the basis of the density of the points and in particular field operations present high point densities due to the low ground speed of the combine while on road operations present low point densities due to the high ground speed of the combine. The DBSCAN algorithm [41] as reported by the authors, requires two input parameters: one is the neighbourhood radius and the other is the minimum number of points. The set of these two values should reflect the density difference between road points and field points. The adoption of a DBSCAN method to perform a clusterisation allowed a possible misclassification of the dataset points when the GNSS points density on the road is similar to the density on the field and vice versa. The first case occurs when the vehicle slows down or stops on the road, while the latter occurs when the GNSS signal was lost. So to reduce these misclassifications, Chen et al developed a direction-distribution-based inference which was based on the idea that the strips in the same field were parallel, with this assumption the authors developed two inference rules. For the former, in case the number of GNSS points is lower than a threshold value, the field cluster was considered a false field. For the latter, the methodology was different as well as the assumptions. Indeed, road segments are consecutive, so the algorithm performed three checks:

- Speed check: if the segments are in a field their speed should be similar otherwise the segments are on the road. To perform this check the authors set a threshold value.
- Direction check: if the segments are in a field their direction should be parallel otherwise the segments are on the road. To perform this check the authors set a threshold value.
- Shared parallel zone check: if the number of parallel segments is greater than a threshold value the segments are in the same field.

With these corrections, the accuracy of this approach is roughly 95% as stated by the authors. The solution can be suitable to perform the automated field boundary identification in this analysis because the method does not require a great computational capability and it can be easily applied to the created dataset to perform the field clusterisation.

Another study investigated is based on a combined use of the DBSCAN algorithm and an object detection (OD) methodology. The latter consists of a methodology to perform object localization in a given image and determine to which category each object belongs. This solution, proposed by Zhang et al.[42], result as an improvement of the analysis performed

by Chen et al, in which the GNSS data were recorded during wheat or paddy harvesting. The procedure to perform the data cleaning and the clusterisation is the same as proposed by Chen et al [37] but instead of performing a Field2Road-Cluster and a Road2Field-Segment the authors in this case decided to adopt an object-detection-based-clustering. The authors investigated three different object-detection-based clustering, such as YOLO V4, Swin-SMask R-CNN and Dynamic R-CNN, in this case, the approach results are quite different from the DBSCAN. Indeed, each trajectory of the dataset was converted into an image and split into two categories: training images and test images. Once the training step was completed, the authors started the clusterisation of the data in roads points and field points. After that, Zhang et al, used a Davies Bouldin index [43], this index analyse the efficiency of the clusterisation by using quantities and features intrinsic to the dataset. The authors stated that the proposed methodology was to identify the field and the road for the acquired dataset as long as is chosen the correct object detection model for the analysed dataset. The methodology proposed by Zhang et al, turns out to be easily applicable to different datasets and can be easily used in this analysis as first stage of identification of the worked fields.

Another investigated solution by using the information provided by the GNSS receiver is based on a developed algorithm based on different assumptions in which, the most important among these is the fully-automaticity of the solution. The solution, proposed by Zhang et al [44], as said before use the GNSS data acquired during the harvesting seasons 2014 and 2016 in Colorado, the authors mounted on each vehicle involved in harvesting, a Nexus 7 tablet running an Android app developed by them to record all the GNSS tracks. In this case, to start or stop the recording the operator had to press a button on the tablet's screen. This approach was based on the development of an expert system to perform the in-field classification, an expert system is a particular kind of artificial intelligence that permits to the computer to simulate human decision-making [45]. In order to perform the autonomous in-field classification, the authors implemented two kinds of rules, in which the first was needed to perform the on-road task recognition while the other one was needed to perform the "road extension", which means being able to classify all the GNSS points found on the same road can be classified surely as road. As reported by the authors, by setting these two rules, the expert system could classify most of the data as on-road points so the remaining points could be classified as in-field. The rules definition proposed by Zhang et al was based on two main rules, the first was that combine harvesters travels faster on the road than on the field due to the surface condition, so a speed rule could easily distinguish fields from the roads. The second rule was that roads are straight or shaped by straight segments, especially in areas with large fields and it was used for road extension. The authors explained that the

main rules that allowed correct classification of the GNSS points were related to the speed performance, the density of points and the quasi-collinear propagation. As reported by the authors, the expert system started the analysis to perform the points classification by checking the speed values and if these were higher or equal to the threshold value for the road identification, the algorithm classified the points as on the road. After the first recognition of the road path, the algorithm started a scan through the time to check for other points that could be classified as roads. The authors explained that if between two road segments, there was a subsequence of GNSS point with a lower speed compared to the previous and the following roads segments, the system automatically checked the duration of this subsequence and if the time span was smaller than the set one, those points were classified as points in which the combine's temporary slowdowns on the road. As reported by the authors, those points represent temporary slowing-down moments which might have occurred due to stops due to the traffic lights or stop signs. After the identification of the road segments, the algorithm started a density test to find low-speed subsequences that are still unmarked, if the system find any subsequences, it considered the points as a new road and started the road propagation as before. As found by the authors, these identified subsequences not always are roads so to reduce misclassification problems a validity test was performed; the test developed by Zhang et al consists into a check if the sequences are surrounded by other unmarked points. The proposed algorithm at the end of the classification of the points on the road or field uses the α-shape function to perform the field boundary identification [46]. This function is required to define the value of the alpha radius, which represents the smallest radius that produces an alpha shape that encloses all points. The authors explain that to compute the correct alpha radius, they used the formula for the Radius of Circumcircle in which were used the header width and the distance between two consecutive GNSS points. To the calculated value, it was added twice the circular error probable (CEP) of GNSS receiver's. As found by the authors, the α-shape function estimated field boundaries smaller than the real ones. To solve this problem, the authors applied an extension of the α-shape by half of the combine's header width, these was possible by applying an improvement of the algorithm proposed by Layton [47]. The solution proposed by Zhang et al results easy to update in each agricultural vehicles, and the capability of the system to identify fields boundaries presented a high-rate success in addition, as reported by the authors this model could also detect boundaries of very irregular fields.

1.3.3 Evaluation of the performance of combine harvesters

Evaluation of the performance of the machinery is the last phase in the planning and control cycle for a field operation and it consists in comparing the planned operation and the actually executed operation [48]. The importance of the performance evaluation is related to the fact that farmers, but also agricultural managers have to take select the machinery for performing a specific activity. Indeed, the effect of this decision can positively or negatively influence the revenue at the end of the growing season. Thus, knowing the efficiency of each machinery can increase the planning capability and consequently the business profit. In accordance with the above-mentioned statements, researchers tried to evaluate the performance of agricultural machinery with increasing accuracy and for this reason, the performance evaluation of different agricultural machinery can be calculated in many ways and each one of the adopted methodologies can be considered globally right. Because performance evaluation in agricultural machinery represents a hot topic, this investigation ranged not only on combine harvesters but has explored the topic more in general by considering also studies on tractors since they are by far the most used machine in agriculture, and therefore many studies are based on analyzing the performance of these machines.

The first identified analysis was performed in 1995 by Hunt D. and Wilson D., where they discussed the performance evaluation of agricultural machinery in their book entitled Farm Power and Machinery Management [49]. The authors dedicated the entire first chapter to this topic and defined the concept of capacity for agricultural machinery. In particular, they pointed out that the capacity calculated for a tractor should be different than that of combine harvesters. This is true because, combine harvester capacity cannot be considered only as area per time, but due to the fact that this machinery processes a certain amount of material and separates desired material from undesired one. Moreover, this book reports the definition of theoretical and effective capacities. The former represents the capacity of the machine in the event that the machine operates continuously and always at the same header width, while the latter is the one that the machine reach in real-world conditions. The authors explained that the effective efficiency of agricultural machinery is a parameter that cannot increase proportionally with the width of the machinery or of the implement, but it is strictly related to the following parameters: machine manoeuvrability, field patterns, field shape, field size, crop and soil conditions. Moreover, for combine harvesters, also the yield must be considered since considering only field capacity is reductive Indeed, as stated by Hunt D. and Wilson D., to obtain an high-efficiency farmers and operators have to test and judge the

crop and the soil conditions as fast as possible, without reducing the quality of the performed operation.

Another approach is that proposed by R. D. Grisso et al. [50] consisting in evaluating the field efficiency of planters and of combine harvesters. In particular, they calculated the field efficiency as the ratio between the theoretical time required to complete the operation and the measured time to complete the operation; Grisso et al have explained that the data about the theoretical time was obtained by finding the ratio between the field area and the theoretical field capacity, while field size was derived from crop yield and knowledge of average crop yield. As found by Hunt and Wilson also the analysis performed by Grisso et al showed that the field efficiency was related to the working speed and at the same time to the field shape. The authors also found out that the working speed at the field contour was lower at approximately 1.6 km h^{-1} than the speed on straight rows, and the delay on field edges was twice longer than those on straight rows but the time spent on edge and straight patterns was the same. In addition, the authors found that the field efficiency on the field edges decreases more during harvesting than during planting [50]. The analysis performed by Grisso et al showed that the evaluation of efficiency performance, especially during harvesting, is not easy to perform because it is related to several factors that are related to the characteristics of the harvested fields. Pitla et al.[51] monitored a four wheels drive tractor (4WD) and a mechanical front wheel tractor (MFWD) to determine the field efficiency of agricultural machinery. The 4WD performed fertilizing and cultivating activities while the MFWD was performing planting activity. In this study, the authors decided to monitor the signal with the information about the tractor fuel rate identified as Liquid Fuel Economy (LFE). This message contained the information about the fuel consumption and it could be used also to estimate the engine load. The authors calculated the field efficiencies by using the working period of the machine intended as the period in which the implement was working or engaging with the soil, and they considered the dwell period (DP) as the period in which the implement was not performing any useful work such as headland turn, refill, etc. The authors also showed a methodology to identify the working and the dwell period by identifying a threshold fuel rate (TFR). The identification of this parameter could be achieved by calculating the draft force and the specific fuel consumption with the methodology proposed by ASAE in their standard D497.7. In this standard, the draft force was obtained by considering the soil texture of the monitored fields, machine-specific parameters, the width of the implement and the tillage depth of the implement. Thanks to this equation the authors stated that the tractor was in a working condition whenever the engine load was the minimum required for the draft power of the implement. They also

showed a methodology to calculate the draft power of each implement by multiplying the operating speed with the draft force. Moreover, the authors calculated the specific fuel consumption and the obtained draft power was converted into the equivalent power take-off (PTO) power by using the tractive efficiency factor for the 4WD and the MFWD. As reported by the authors, the computed PTO power was then used to calculate the specific fuel rate that was used as TFR[51]. The authors showed that the field efficiency could be deducted by analysing and monitoring the fuel consumption and that it was easily influenced by the kind of operation performed by the machinery. The methodology proposed by Pitla et al. was suitable for computing the performance evaluation of tractors performance by monitoring the fuel consumption, and this approach can be surely adopted to monitor the combine harvester performance evaluation.

Layton et al. proposed a methodology to evaluate the harvesting performance by monitoring multiple combine harvesters that have worked in the same field. Firstly, the authors identified each portion of the field harvested by each one of the combines and subsequently various metrics were computed for evaluating the combine efficiencies. One of the investigated metrics was the field efficiency and it was computed as the ratio between the harvested area and the travelled distance multiplied by the header width. The harvesting efficiency obtained in their analysis provided a logical matrix with values between 0 and 1 that represent the average fullness of the combine's header. The authors identified also the moments in which the combine's header was empty such as during moving to reach the field edge to unload and this time can influence negatively the combine's performance. So, the previous formula proposed by the authors should be changed in order to consider only the situation in which the combine's header result totally full. The authors reported that with information about the grain flow and header position, it could be possible to estimate the harvesting performance more precisely.

Another metric that was calculated by the authors, was called non-harvest percentage, which was computed as the percentage of the time in which the combine was on the field but not performing harvesting. The information provided by the non-harvest percentage result crucial in the analysis, because the evaluation of combines cannot be restrained to pure harvesting operations on fields but should also comprise non-harvesting operations. By performing a deeper analysis of the data, the authors found out that the header of the combine rarely reached the full condition of 100%, so the threshold value to consider the header full was lowered to 90%. With this new adjustment proposed by the authors, the efficiency analysis has taken into account only the amount of time in which the combine was performing harvest, and this metric was called adjusted full-harvest percentage [47]. The

proposed solution by Layton et al. introduced different metrics to evaluate the harvesting performance of combine harvesters based on what kind of inefficiencies, in a specific moment, the user wants to be addressed. This approach deeply evaluated the activities performed by combine harvesters during the on-field activities and identified all the parameters that could introduce inefficiencies, but the authors did not take into account the amount of crop harvested that in combine harvesters result an important parameter.

Another approach studied to evaluate the performance of agricultural machinery was proposed by Zhou et al., in which the authors first broke down the on-field activity into two parts denoted as productive and unproductive. The authors considered productive only the harvesting activity, while considered un-productive the turning times, in-field preparations, adjustments, in-field transport time, unloading, etc.

From the former, the authors extracted the coverage area, which they considered as the area in which the agricultural machinery performed the activity and split it into other two parts called headland and field body area. Inside these two sub-parts, the authors identified several headlands passes (H) and field-work tracks (T), so the authors were able to calculate the distance-based field efficiency. Zhou et al considered the distance-based field efficiency as a function of the field shape, the machinery features, the working width and the fieldwork pattern. The methodology proposed by the authors to compute the distance-based field efficiency is related to the ratio between the total effective length of the headland passes and of the tracks and the total length of continues passes [52]. The authors also performed an analysis to show the degree of dependence of the field efficiency on the operational features. The proposed methodology allowed the identification of a new index to monitor and evaluate the field efficiency of agricultural machinery, in which the index is strictly dependent to the field, machinery and operating features. As observed for the methodology proposed by Layton et al. this approach is able to identify the field efficiency of agricultural machinery, but the metrics presented by the author do not take into account the harvesting performance of combine harvesters.

Chapter 2

2 Materials and Methods

2.1 The proposed methodology

The proposed methodology includes a mix of approaches investigated throughout three years. The decision to split the investigation into three parts was forced by the complexity of the harvesting activity, in which different entities were involved such as combine harvesters, fields and crops. For this reason, this chapter was divided into several parts; the first is dedicated to the description of the monitored combines; while the others are dedicated to explaining the adopted methodologies for data acquisition, tasks identification, field boundary identifications, and performance evaluation.

2.1.1 The monitored combine harvesters

For the monitoring of combine harvesters, an agricultural contractor was searched in Bologna's Province. The choice of limiting the search to the Province of Bologna was related to the fact that the acquired data needed to be frequently and manually downloaded from data loggers and that eventual unexpected events should be easily dealt with. The selected agricultural contractor had the following characteristics:

- managed more than 1000 ha leading to data with significant variability.
- Owned combines equipped with a CANBUS network permitting ease of the acquisition of data for calculating combines' performance.
- Performed harvesting activities during the entire season (from June to October) and this requirement was necessary for acquiring data related to different crops.

The selected agricultural contractor owned two New Holland CR 7.90 combine harvesters (CNH Industrial N.V., Amsterdam, NL) as shown in Figure 2.1.

Figure 2.1: Photo of one of the monitored combines before starting the workday

The specifications of the combines are reported in Table 1, and they were equipped with sensors that simplify the operator tasks and at the same time could provide useful information thanks to their embedded sensors. The two combines were denoted as C1 and C2, respectively. This choice was made in order to monitor what occurs on a farm during an entire harvest season.

Table 2.1: Specifications claimed by the manufacturer of the combine harvesters used in this analysis.

Maximum engine power	(kW)	338
Engine displacement	(cm^3)	8700
Number of cylinders	(-)	4
Engine emissions	(-)	4B
Weight	(kg)	18000
Cutting bar width	(m)	7.62
Reel diameter	(m)	1.07

2.2 Data acquisition

The data acquisition was performed during two harvesting seasons, in 2020 the dataloggers were mounted on the combines from 21/06/2020 till 31/10/2020, while in 2022 they were mounted from 21/06/2022 till 18/10/2022. The combines were monitored in this period because, in the area of Bologna, the harvesting of wheat and barley began in late June while the harvesting of soybean ended in late October. The dataloggers installed on the two combines were equipped with two CANBUS channels, compliant with the standards SAE J1939-14 [53] and SAE J1939-15 [54] permitting the acquisition of the signals coming from the CANBUS network. The datalogger embedded a GNSS receiver without differential correction and with a claimed CEP of 2.5 m which permitted to measure the combines' positions and speeds. In order to simplify the operator's activities during harvesting, the dataloggers were set up to automatically acquire all the CANBUS messages whenever the combine's engine was turned on. The data acquired were internally converted into ASCII format and temporarily stored in the datalogger's memory. Approximately every month, the data were manually downloaded and uploaded on a Network Attached Storage (NAS) for the following reasons:

- Create a backup of the acquired data.
- Create a historical database in which to store all acquired data sets for future analysis.

From all the acquired signals, it was selected only those which permitted the extraction of the information necessary for improving combines' management. In particular, the signals used to perform this analysis were reported below:

- Engine Reference Torque: that reports the maximum torque that the engine could deliver and it is denoted as T_{er} in the following.
- Actual Engine Percent Torque: that is the calculated output torque of the engine as inner torque, as a percent of T_{er} and it is denoted as T_{ae} in the following.
- Nominal Friction-Percent Torque: that reports the frictional and thermodynamic loss of the engine itself, pumping torque loss and the losses of fuel, oil and cooling pumps as a percent of T_{er}, and it is denoted as T_{nf} in the following.
- Engine Speed: that reports the revolution speed of the engine crankshaft, and it is denoted as n_e. The sensor to monitor n_e is located on the crankshaft and it provides to the ECU the position of the pistons inside the bore. With this information, the ECU can control the fuel injection and start the sparks ignition events at the right moment; The sensor normally adopted is based on the "Hall effect". In particular, the sensors

can read a trigger wheel made from a ferrous metal, in the wheel there are one or more missing teeth and every time the tooth passes in front of the sensors will change the signal sent to the ECU (Figure 2.2).

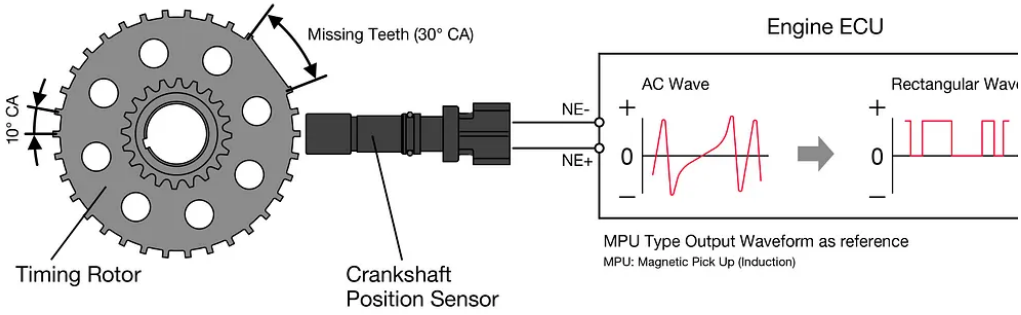

Figure 2.2: Operating scheme of the engine speed sensor [55]

This information in addition to the knowledge of the total number of teeth on the wheel can calculate the engine speed. These sensors are usually mounted very close to the crankshaft such as the crank pulley, the timing gear or on the flywheel.

- Engine Fuel Rate: that reports the fuel consumption of the engine, and it is denoted as $\dot{F}_r$ in the following. The value of the engine fuel rate is an important parameter that helps farmers and agricultural managers in their management decision, but it could not be directly measured by a sensor. Indeed, it is indirectly calculated by the manufacturer from the "fuel mapping".
- Header Down: that reports the position of the combine header and it is a logical signal and is 0 when the header is up and 1 otherwise. It is denoted as H_{dd} in the following. The header or cutter bar of a combine harvester is composed of different parts depending on the kind of cutter bar, but each one has a sensor that monitors constantly the position respect to the soil. This sensor consists basically of a potentiometer, a system that with the rotation around an axis can change the resistance and consequently the voltage drop as shown in Figure 2.3.

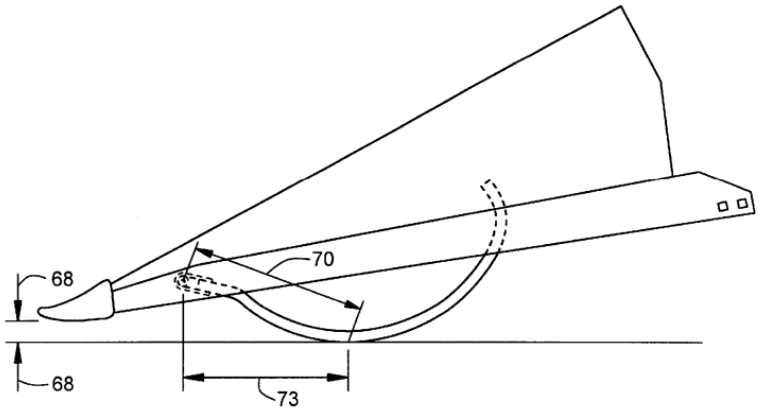

Figure 2.3: Side view of the header snout with the sensor arm at a low operating setting [45]

Under the header and in lateral position there were two arms, in which one end of the arm touch the ground whenever the header was in a down position while on the other end, the arm is connected to the potentiometer.

- Crop Flow: that reports the flow of harvested crops per unit of time, and it is denoted as $\dot{C}_f$ in the following. The grain yield sensor is a sensor that could monitor the amount of grain that is collected in the combine, this is possible by measuring the amount of clean grain that enters the grain tank in a specified period of time ($1 \div 3$ s). The two monitored combines embed a yield sensor that measures indirectly the flow from the impact force of the grain on a sensing plate. This sensor is composed of a jointed bar with a sensing plate at one end and a counterweight at the other end, in order to exclude the rubbing effect of the grain as reported in Figure 2.4.

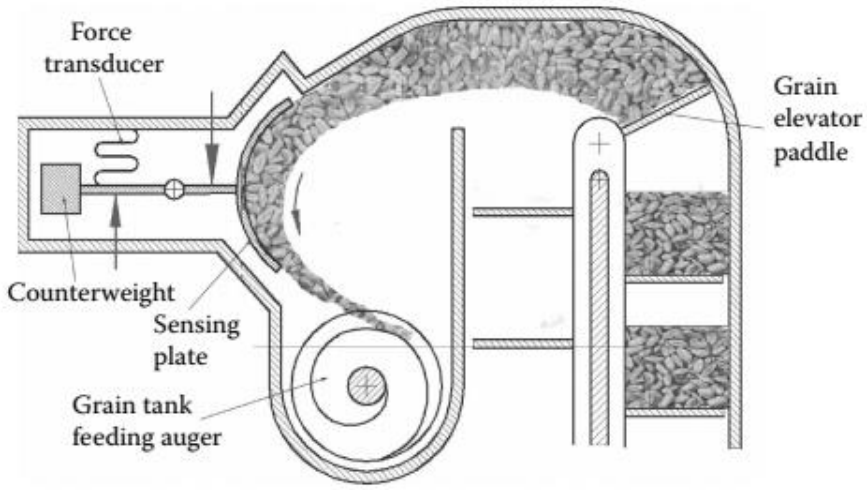

Figure 2.4: Graphic scheme of the grain yield sensor embedded in the monitored combines [1].

- Unload Engine Auger: that reports the auger's engine status, it was 0 when it was turned off and it was 1 otherwise. It is denoted as U_{EA} in the following. The sensor measures the state of the engine auger, consisting of an electro valve that activates a double-acting hydraulic piston that pushes a tension pulley and activates the engine.
- Navigation-Based Vehicle Speed: reports the speed of the vehicle expressed in kilometres per hour, and it is denoted as V.
- Compass Bearing: that reports the direction of the movement of the vehicle expressed in degree, and it is denoted as α_{CB}.

2.3 Data analysis

In this section, it is reported in detail all the analyses performed on the acquired data. The chosen programming environment for developing the algorithm for the data analysis was MATLAB® (MathWorks Inc, Natick, Massachusetts, United States). The acquired dataset, to be processed was converted into a .MAT file by using an ad hoc MATLAB script. The MATLAB script required the dataset and the CAN (DBCs) databases. A DBC is an ASCII file required to perform a decoding of the raw CANBUS into physical values and for this study, the following DBCs were used: J1939 [54], ISO 11783 [56] and the DBC of the GNSS receiver. Firstly, from the analysis, acquisitions shorter than 20 seconds were excluded. This choice helped to exclude erroneous data where the combine was shortly turned on by mistake. Moreover, the data were cleaned, in order to exclude erroneous data occurring in cases where the GNSS receivers were unable to connect to the satellites, such as when the combines were located close or inside to sheds. This preliminary data cleaning was performed through a manual identification of the errors detected by plotting the values of the derivative of latitude, longitude and altitude. Values above a certain threshold (i.e. greater than 4 and equal to 0)were excluded from the analysis. Figure 2.5 shows the trends of latitude signals before cleaning (in blue) and after cleaning (in red) with the before mentioned approach.

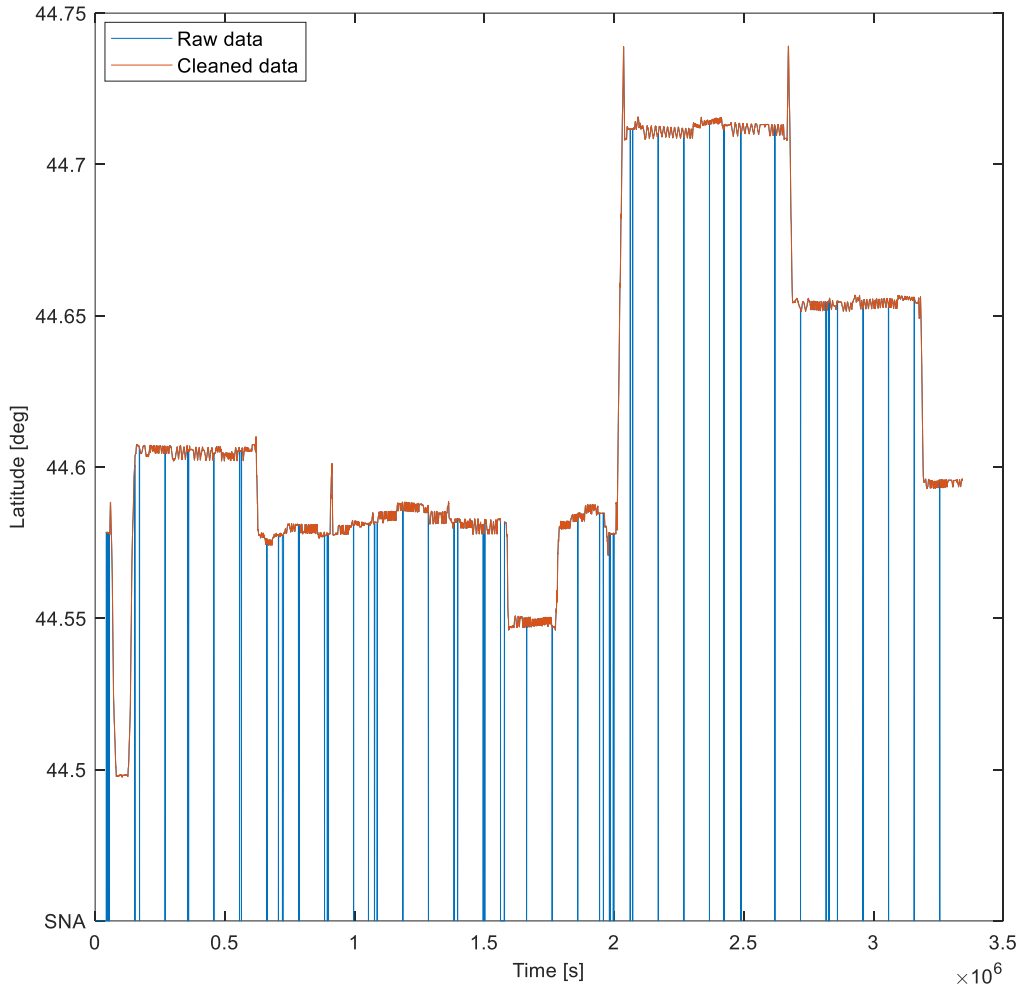

Figure 2.5: Trend of the latitude signal acquired from the GNSS receiver (in blue) and trend of the latitude signal after the cleaning

Then data were smoothed with a filter with the purpose to reduce the positioning error caused by the used GNSS receiver, which caused a jittering of the recorded track. This error was reduced by applying the MATLAB embedded function called “sgolayfilt”. This function performed a filtration of the dataset, as reported by Heiβ et al [57] in their analysis, by applying a Savitzky-Golay filter. Similarly to Heiβ et al, the polynomial order was set to one because it fitted the chronological order of the dataset, while it was determined that a frame length of 25 would provide a smoothing that adequately represented the combine's track. In Figure 2.6, it is shown in blue the trend of the latitude’s signal before the filtering, while in red was shown the trend of the latitude after the filtering.

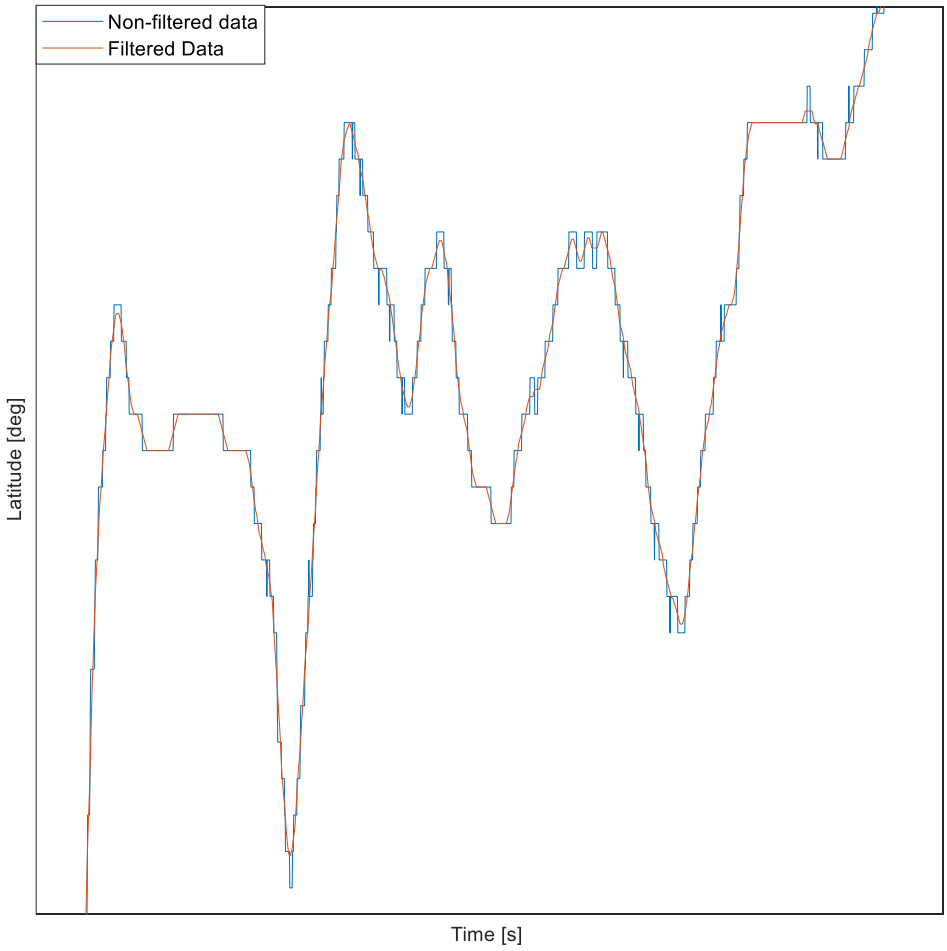

Figure 2.6: Trend of the latitude signal not filtered after the adoption of the Savitzky-Golay filtering

2.3.1 Automated task identification

The approach to performing the automated task identification was similar in principle to that proposed by Mattetti et al [19] where two different kinds of classification of data samples were adopted. A first classification was performed based on the combine's position and it was possible thanks to two shapefiles downloaded from the Geoportale of the Emilia Romagna's Region [58] which contained documents, and make usable cartographic data and services of the Emilia Romagna Region. From these shapefiles, it was possible to extract different information useful to perform this analysis. In the first shapefile, there were all the polygons, classified on the basis of the land use, of the Bologna's Province. While a third shapefile was created by using the QGIS platform (Open Source Geospatial Foundation Project, http://qgis.osgeo.org) a Geographical Information System and it contained. For the purpose of the analysis, only the polygons classified as agriculture (i.e., denoted as "AGR" in the attribute table) were selected. The second shapefile contained all the road segments of Emilia Romagna's region, while the third contained information about the location of the

farm's site. In order to limit memory usage, only the polygons enclosed in a bounding box of 60 km around the Bologna's Province, coinciding with the farm site and on this bounding box were clipped the land use and the road shapefiles. Thanks to this geographical information and by using the MATLAB embedded function called "inpolygon" and by developing an ad hoc function, the GNSS's points classification was carried out. The first function permitted to classification of the position of each point inside or outside a polygon, while the latter was able to classify all the points if they are close to the road's segments. Thanks to these functions, points were classified into one of the following categories (Figure 2.7):

- ***Road:*** every time the combine's position was closer than 3 meters from any road stretch. This threshold was chosen based on the CEP of the GNSS receiver utilized in this study.
- ***Field:*** every time the combine's position was inside the boundary of any field plot.
- ***Farm:*** every time the combine's position was inside the boundary of any farm site.

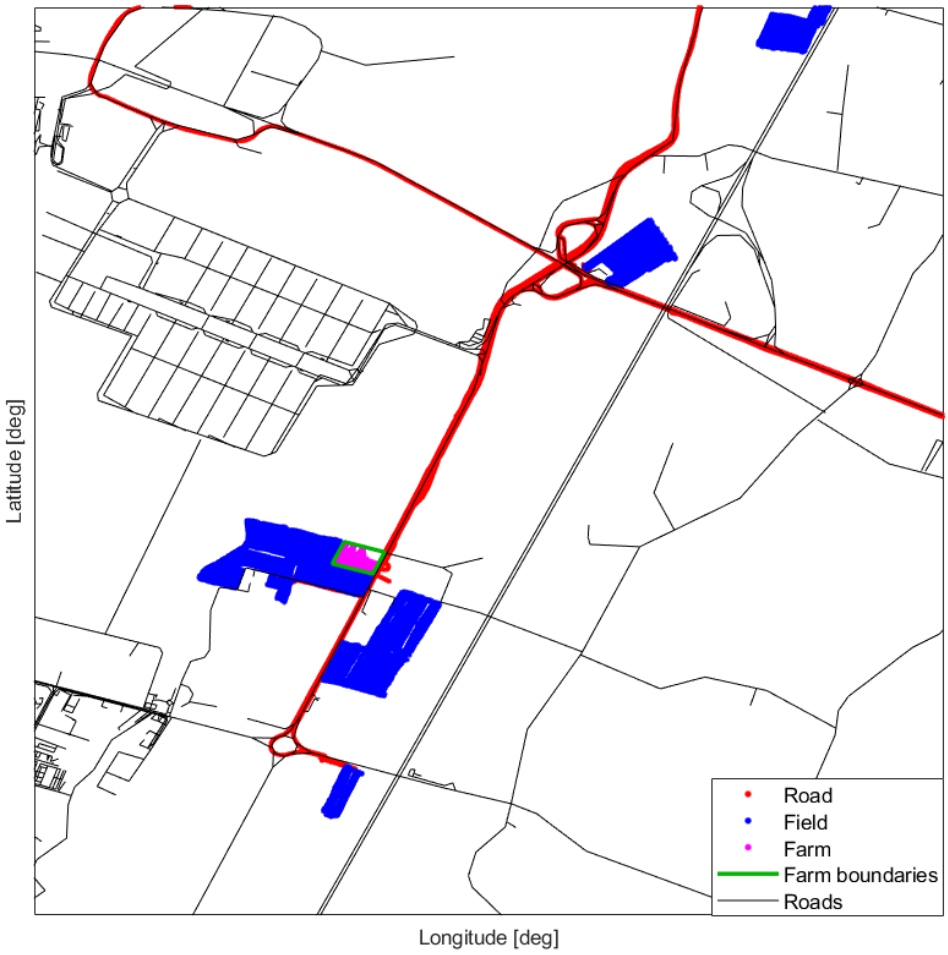

Figure 2.7: Automated identification of the GNSS points on the basis of the three identified combines positions on the road, at the field, and at the farm.

After that, data samples were classified into one of the possible tasks in which combines are usually involved. In particular, seven tasks were defined which were: idle at farm, idle at field, transport on road, transport on field, work, unload, unload and work. The logical rules of these tasks were reported in Table 2.2. Combining H_{dd}, V and C_f with combine's trajectory, the distance travelled during work (D_h) and during other tasks (D_{nh}) were calculated. For fields operations, D_h and D_{nh} represent respectively the length of the passes and of the headlands. These parameters depend on several operational parameters such as the length of the field, and the kind of headland performed by the operator [59]. During headland turns, the maximum distance travelled by the combines was equal to double the width of the header, which was 6.72 m. The algorithm started by calculating the series of D_h and D_{nh} based on the position of the header. Then the headland duration Δt was calculated as the time elapsed between the falling and the rising points of H_{dd} signal (Figure 2.8).

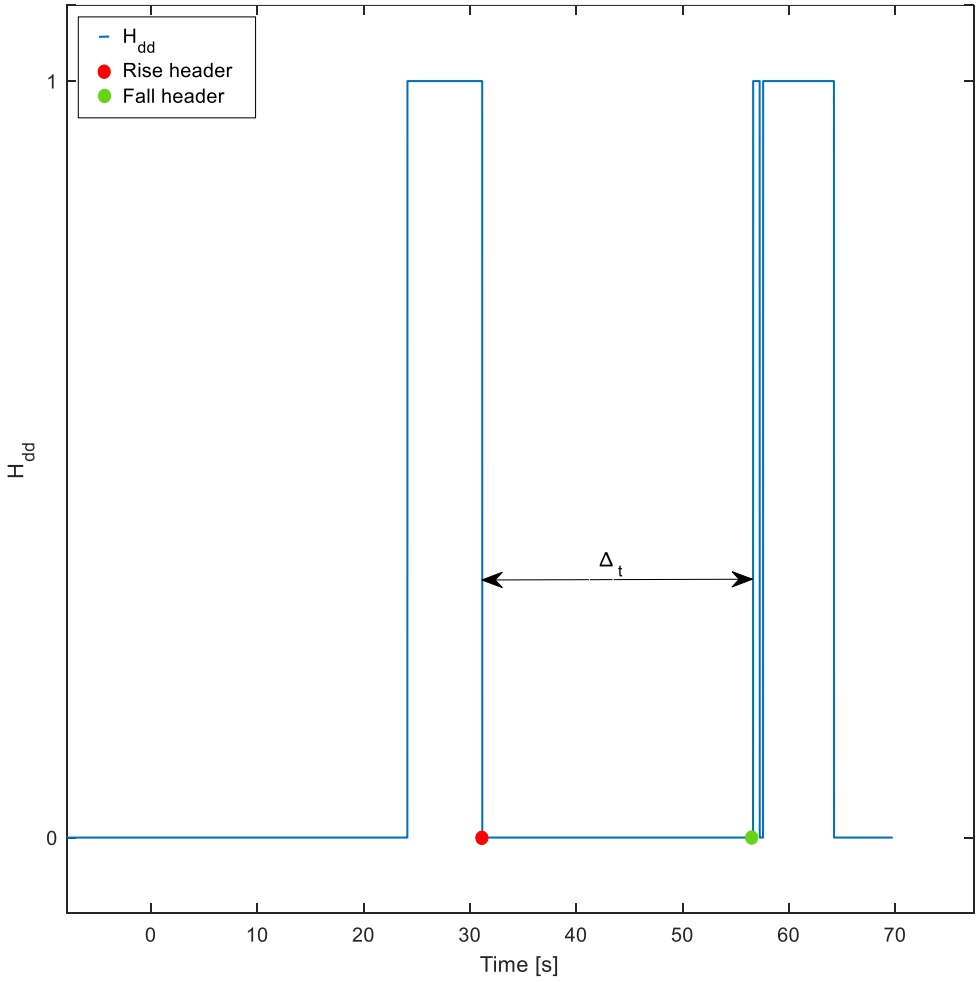

Figure 2.8: Graphical representation of the chosen methodology to compute the headland turn duration

Table 2.2: Rules adopted for the identification of the operative states of combine harvesters

Operating status	Combine position	Boolean operator	Combines operating activity
Idle at farm	Farm	AND	$V = 0\ km\ h^{-1}$
Idle at field	Field	AND	$V = 0\ km\ h^{-1}$
Transport on road	Road	AND	$0<V\ km\ h^{-1}\ and\ C_f = 0\ g\ s^{-1}$
Transport on field	Field	AND	$0<V km\ h^{-1}\ and\ C_f = 0\ g\ s^{-1}$
Passes	Field	AND	$V \leq 7\ km\ h^{-1}\ \ and\ C_f > 0\ g\ s^{-1}\ and\ Hdr_{Dn}$=1
Headlands turn	Field	AND	$V \leq 7\ km\ h^{-1}\ and\ \ C_f = 0\ g\ s^{-1}\ and\ Hdr_{Dn}$=0
Unload	Field	AND	$V = 0\ km\ h^{-1}\ and\ U_{EA}$=1 and Hdr_{Dn}=0
Unload and Work	Field	AND	$V \leq 7\ km\ h^{-1}\ and\ C_f > 0\ g\ s^{-1}\ and\ Hdr_{Dn}$=1 and U_{EA}=1

The thresholds shown in Table 2.2 were chosen because of in-depth knowledge of the combine components involved in the different tasks. For example, the speed thresholds were identified by starting to consider the simplest activities and those that were going to involve the fewest components. Next, the range of variation for the signals from the different components was identified (e.g., the activation of a component such as U_{EA} varies between 0 and 1). By combining the data that comes from the different components with the time course of speed and position, it was possible to determine the rules that identify the different activities performed by the combine.

Moreover, as stated by Zhang et al. [44] in their analysis, combine harvesters are faster on the road rather than on fields. This assumption can be easily explained because the surface of the road is normally smoother than that of a field. The lowest limit of the threshold value was determined by performing a search on the entire dataset of the lowest speed value reached by the combines during performing the transport condition as shown in Figure 2.9.

A quite different approach was adopted to set the speed threshold value of the work condition and unload and work condition; in these cases, the speed could change from field to field for different reasons such as yields of crops, kinds of harvested crops, eventual presence of obstacles (e.g., trees, high voltage pylons, etc) and the shape of the field. For this reason, it was investigated all the speed values when the combines were on field and where the speed

was close to 1 km h^{-1} the values of longitude and latitude were investigated on the map to evaluate the presence of obstacles.

The definition of these rules allows the algorithm to be able to classify all the data, the GNSS points (Figure 2.10) and the combine's engine performance (Figure 2.11a and 2.11b) in one of the above-mentioned tasks.

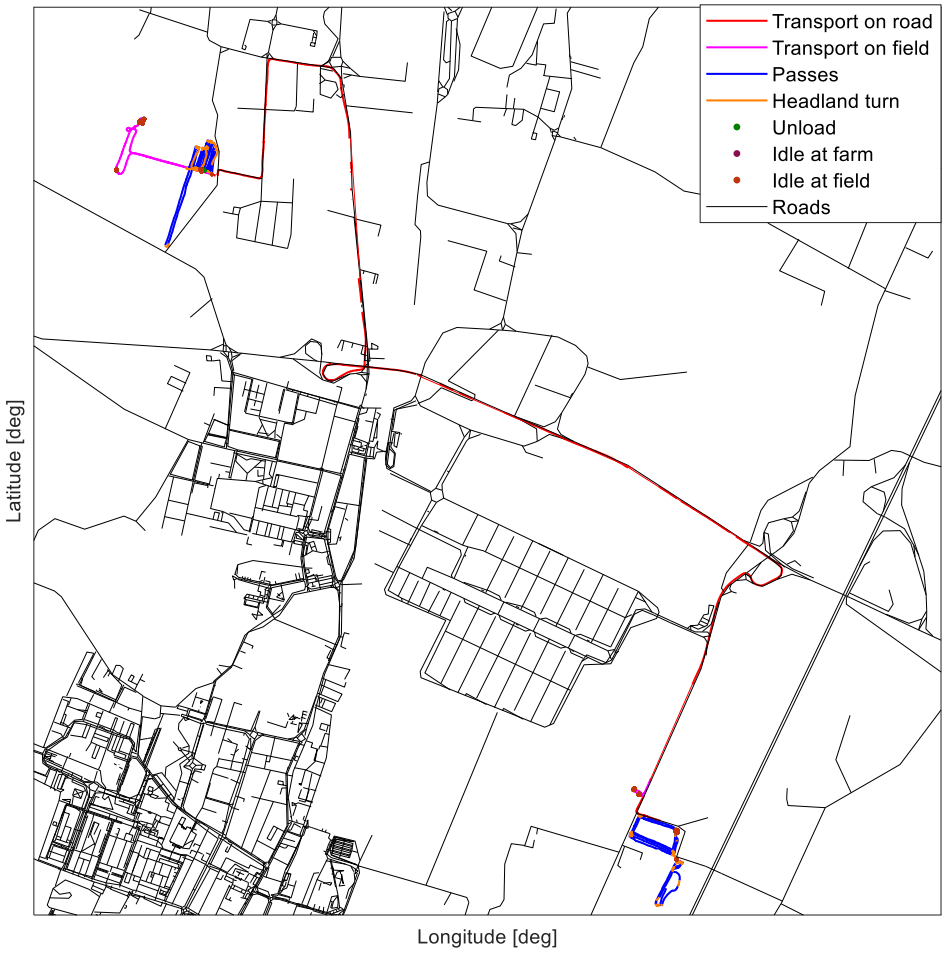

Figure 2.9: Classification of the acquired dataset based on the seven identified tasks

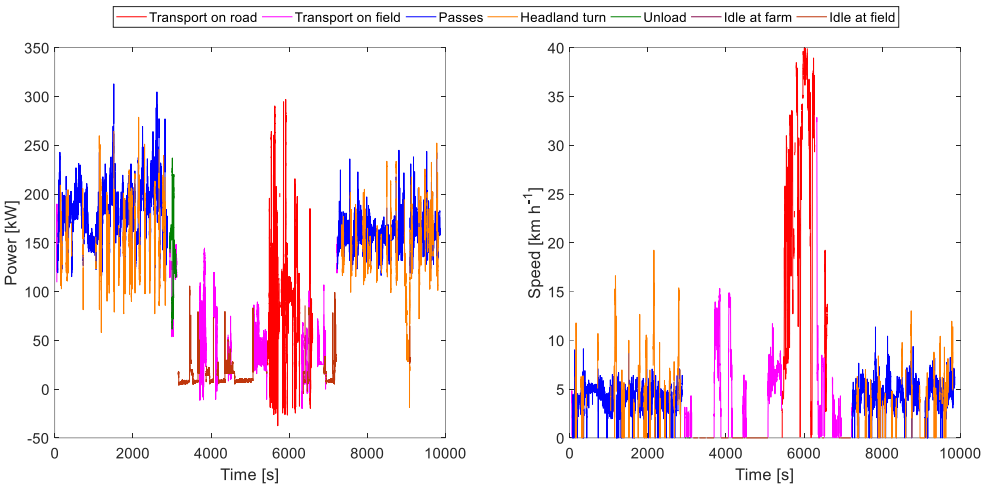

(a) Classification in tasks of the power's trend

(b) Classification in tasks of the speed trend

Figure 2.10: Classification of the power and the speed signals based on the seven identified tasks

2.3.2 Automated field boundaries identification

After having classified the recorded GNSS samples into tasks, those classified as to the passes task were chosen. Thus, this information permitted to identify the shape of fields. Several approaches for the automatic field boundaries identification of the harvested fields were identified in the literature, but those that proved to provide the best results were based on the DBSCAN algorithm [42]. Before starting from the clusterisation, it was mandatory to individuate the position of the left and right outermost points of the combine's header in a pass in order to compute the corrected value of the harvested area. The calculation of the coordinates of the right and left outermost points of the combine's header could not be performed with the coordinates of the GNSS points expressed in Geographical coordinates. For this reason, was applied the MATLAB embedded function called "latlon2local" to convert the point location expressed in latitude, longitude and altitude from Geographical coordinates to Cartesian coordinates expressed as x_{East}, y_{North} and z_{Up}. In order to be able to perform this conversion the function required to set the origin of the coordinates; in this analysis it was chosen as origin the coordinates of the farm site.

Considering that the GNSS receiver was placed in the middle of the cabin, with the combine's position, the combine heading angle, and the header width, the left and right outermost points of the header were calculated using Eqs. 2.6, 2.7, 2.8, 2.9. In those equations, x_a, y_a, x_b, y_b represent the coordinates of the right and left outermost points of the combine's header, x_{East}, y_{North} represent the recorded coordinates of combines through the GNSS receiver, W represents the header width and α_{CB} the heading angle calculated by the compass bearing of the GNSS receiver. In particular, it represents the angle between the theoretical straight direction and the real direction of the combine as shown in Figure 2.12.

$$x_a = x_{East} - \frac{W}{2} * \sin(\alpha_{CB}) \tag{2.1}$$

$$y_a = y_{North} + \frac{W}{2} * \cos(\alpha_{CB}) \tag{2.2}$$

$$x_b = x_{East} + \frac{W}{2} * \sin(\alpha_{CB}) \tag{2.3}$$

$$y_b = y_{North} - \frac{W}{2} * \cos(\alpha_{CB}) \tag{2.4}$$

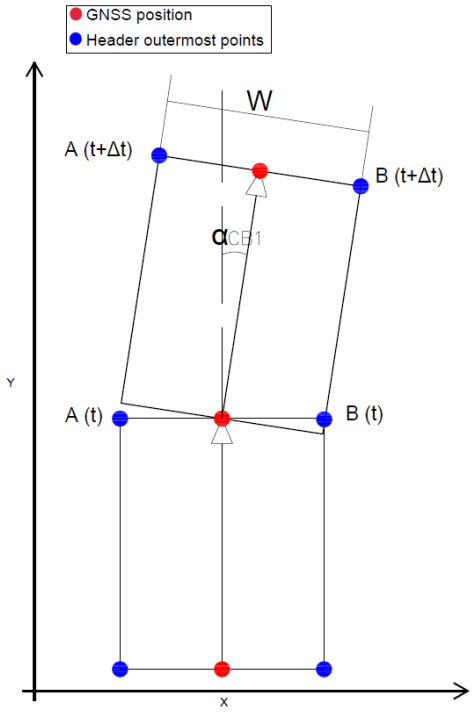

Figure 2.11: Identification of the combine's position and the edge's header position. In blue were reported the header's points, in red the combine's position provided by the GNSS receiver

Once the conversion was performed, it was created a unique array that contained all the coordinates header's points and by using a MATLAB function called "DBSCAN" and it was able to obtain one cluster for each identified field as shown in Figure 2.13.

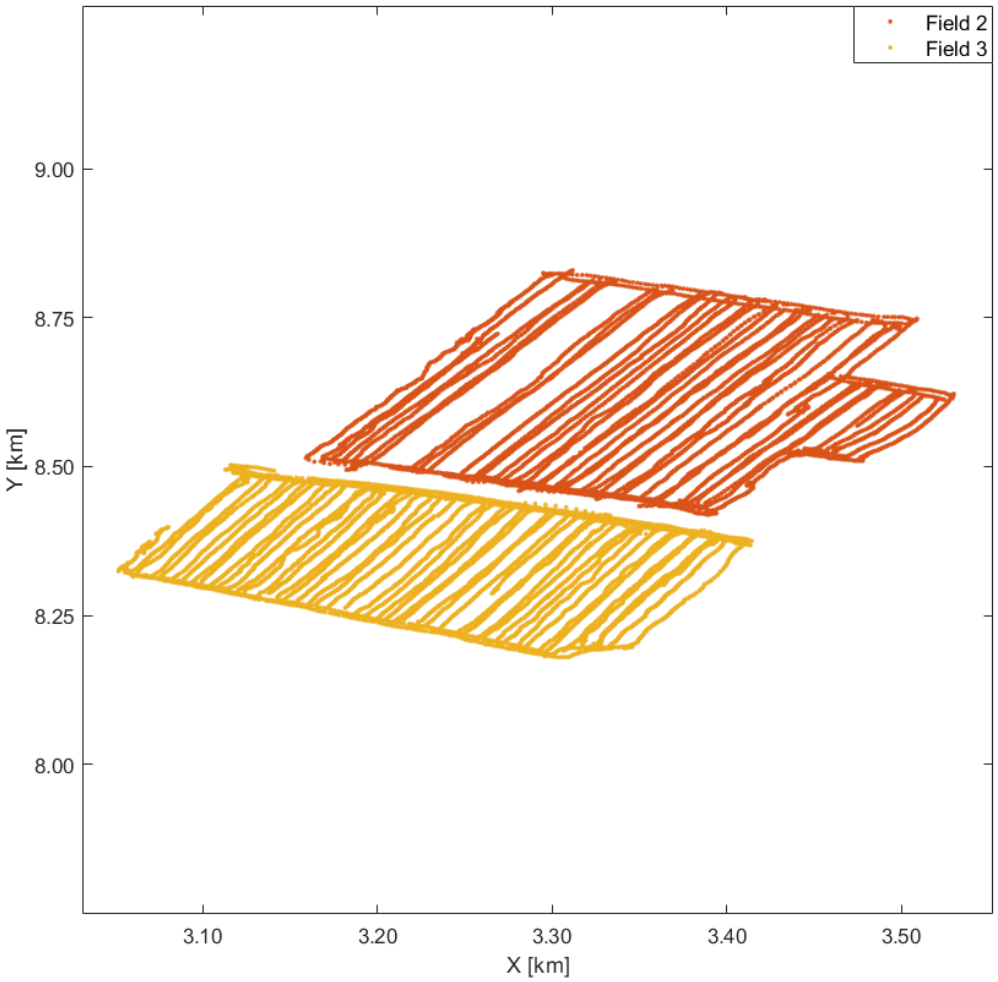

Figure 2.12: Field identification by using the MATLAB "DBSCAN" function

This function was able to perform the cluster identification process and required three inputs, the first is the dataset, the second is the threshold radius to perform a neighbourhood search and it is called *epsilon* and the latter is the minimum number of points required to identify a core point inside the cluster and it is called *minpts*. To perform this analysis *epsilon* was set to 19 and the *minpts* to 9. The value of *epsilon* was set by evaluating the size of the smallest field in the shapefile reporting the boundaries of fields. The minimum detected width was 38 m while the length was 119 m. While the choice of the value of the *minpts* was determined iteratively by choosing the value that allowed the best field identification. Indeed, a lower value of *minpts* did not allow the correct field identification because created several small core points, while a higher value was not able to identify any field.

Once the clustering was done, to evaluate the performance of the algorithm, a shapefile was created using QGIS, in which all the polygons of the collected fields were reported while information about the areas and perimeters of each collected field was stored in the shapefile attribute table. This shapefile was used to perform a comparison visual comparison between

the fields identified manually in the created shapefile and the fields identified automatically by the algorithm.

By using the MATLAB built-in function named alphaShape, it was created a bounding area that enveloped a set of 2D points and the field boundary of each clustered field was extracted. The choice fell on this function because it outperforms MATLAB's built-in function called “boundary” in fields equivalent to non-simply connected spaces (such as in areas containing non-harvesting portions due to obstacles) (Figure 2.13a and Figure 2.13b). This permitted to obtain a more realistic value of harvested area and field capacity of each field as shown in Figure 2.14.

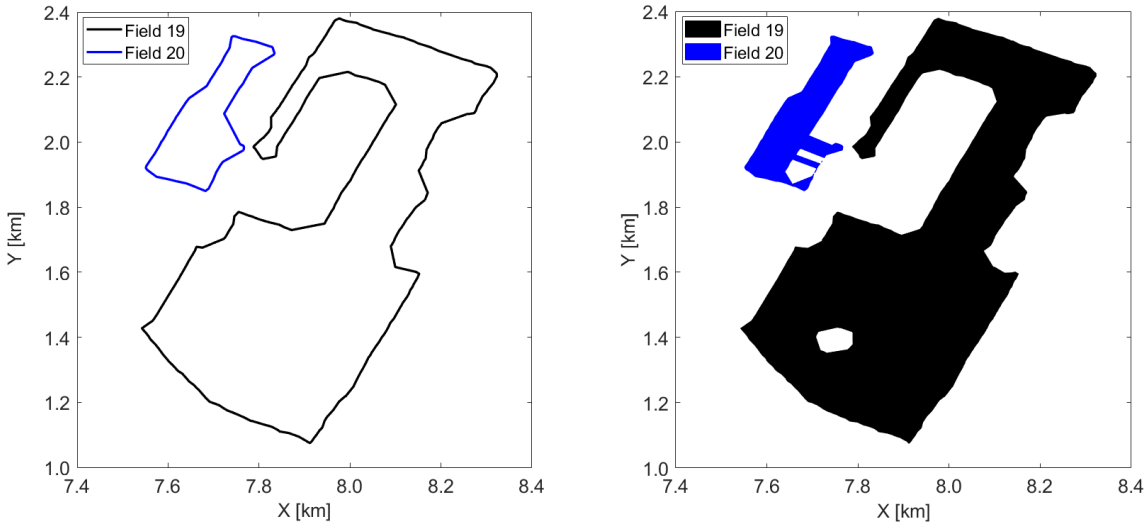

(a) Identification of the field’s boundaries by adopting the function “boundary”

(b) Identification of the field’s boundaries by adopting the function “alphaShape”

Figure 2.13: Comparison between the adoption of the MATLAB fuction "boundary" and the function "alphashape" for the identification of the field's boundaries

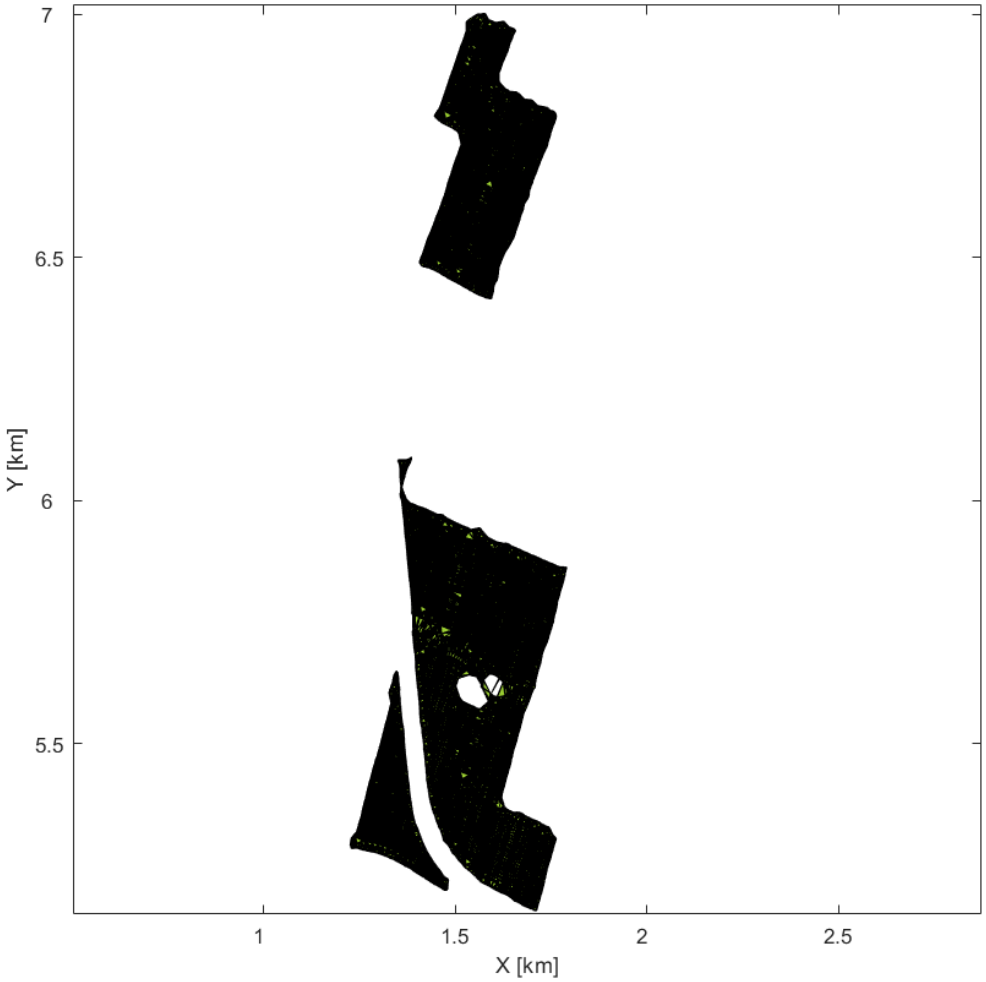

Figure 2.14: Field boundaries identification performed by using the MATLAB function "alphashape"

2.3.3 Combine harvester performance evaluation

Thanks to the information obtained by the algorithms presented in section 2.3.1 and 2.3.2, information about the performance of the two combine harvesters were calculated. In particular, by combining the data obtained from the automated task identification and the data about the field boundaries with the signals that were acquired directly from the CANBUS network of the combines, several performance metrics were calculated for each identified field. With the signals coming from the CANBUS network, the engine power (P_{eng}), the crop yield (C_{Yield}), and the fuel consumption (F_{cons}) were calculated. These were calculated with Eq. 2.5, 2.6, and 2.7.

$$P_{eng} = (T_{ae} - T_{nf})/100 \times \left(T_{er} * n_e * \frac{2\pi}{60}\right) \quad (2.5)$$

$$C_{Yield} = \int_{t1}^{t2} \dot{C}_f \, dy \tag{2.6}$$

$$F_{cons} = \int_{t1}^{t2} \dot{F}_r \, dt \tag{2.7}$$

To perform an analysis of the combine's performance, in each one of the harvested fields and to evaluate how these performances were influenced by the field shape complexity, the area-perimeter ratio φ_{sr} was calculated as the ratio between the field area and the field perimeter squared as reported in Eq. 2.8 [60].

$$\varphi_{sr} = \frac{A_i}{P_i^2} \tag{2.8}$$

Other parameters that needed to be considered in order to perform an analysis of the combines performance are the duration noted as t_i, the field capacity noted as f_{ci}, the crop yield and the fuel consumption per hectare noted respectively as C_{YH} and F_{consH}, the mean power and mean speed noted respectively as $\dot{P}_{eng}$ and $\dot{V}$. The computing of these parameters was reported in Eqs. 2.9, 2.10, 2.11, 2.12, 2.13, 2.14

$$t_i = t_{2i} - t_{1i} \tag{2.9}$$

$$F_{ci} = \frac{A_i}{t_i} \tag{2.10}$$

$$C_{YHi} = \frac{\int_{t2}^{t1} \dot{C}_{fi} \, dt}{A_i} \tag{2.11}$$

$$F_{consHi} = \frac{\int_{t2}^{t1} \dot{F}_{ri} \, dt}{A_i} \tag{2.12}$$

$$\bar{P}_{engi} = \frac{\sum \dot{P}_{engi}}{\Delta t_i} \tag{2.13}$$

$$\bar{V}_i = \frac{\sum V_i}{\Delta t_i} \tag{2.14}$$

In the presented formulas, the parameters i and j represent respectively the number of the identified field and the kind of task performed. Through the comparison between the parameters obtained from the monitored combines with the parameters reported in the literature it was able to monitor the performance of the two monitored vehicles.

Chapter 3

3 Results and Discussions

Organisational remarks

The Results and Discussion chapter is organised as follows:

- **Automated task identification** reports the ability of the algorithm to classify the acquired signals into tasks.
- **Automated field boundaries identification** reports the results of the boundaries of harvested fields and information and the calculation of their perimeters and areas.
- **Combine harvester performance evaluation** reporting the calculated the combine harvesters metrics and their analysis in order to describe how combines were used during harvesting season.

3.1 Automated tasks identification

The proposed algorithm was tested and validated by using the data acquired during the harvesting seasons of 2020 and 2022. In 2020, both combines worked for 51 days (respectively 12 and 39 days) this lower worked time measured for C1, it was related to a mechanical failure on the combine that stop it for maintenance; while in 2022, they worked for 62 days (respectively 40 and 22 days). In 2020, 304 hours were collected; while in 2022, 353 hours were collected. C1 and C2 combines worked for 92 and 211 hours in 2020; respectively; while they worked for 135 and 218 hours, respectively in 2022. The working time accumulated by the two combines in 2022 increased by 21% with respect to that of 2020. This increase is mostly caused by combine C1 where its working time increased by 45% between 2020 and 2022. This increase of the time usage is related to a consequent increase of the harvested fields from 2020 to 2022; indeed, the combines harvested in 2020 and 2022, 54 and 94 fields, respectively. As shown in Figure 3.1a and Figure 3.1b, the classification's algorithm identified eight different tasks in which, combine harvesters were usually involved during harvesting season. The unload and work tasks were intentionally omitted because their contribution was lower than 1%. As shown in Figure 3.1, both C1 and C2 spent most of their time in harvesting which in the graph is reported as on work. Indeed, C1 spent almost 68% and C2 62% of their time performing the on passes task, respectively.

These obtained values are comprised in the range of 60-70% as reported by Savickas et al. [61] .

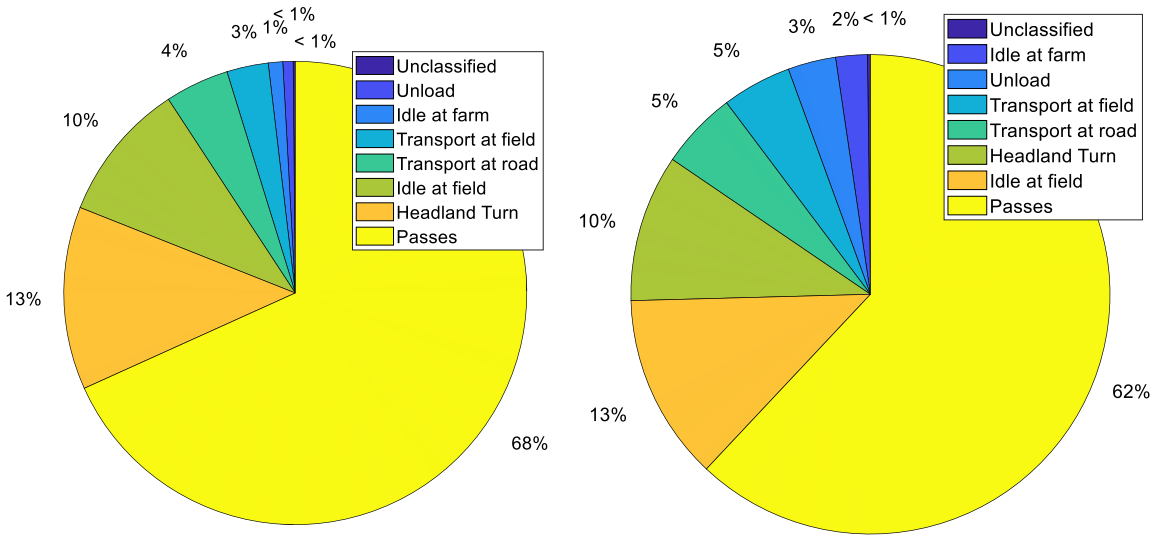

(a) Time contribution of each task on the entire C1 activity

(b) Time contribution of each task on the entire C2 activity

Figure 3.1: Time contribution of each task on the entire combines activity

The time contribution by the two combines in idle conditions was reduced; indeed, in 2020, C1 and C2 were run on idle for 14% and 15%, respectively; while, in 2022, they were run on idle for 10% and 13%, respectively. The time contribution of idle at field results greater than idle at farm because the number of idling stops at field (with a mean duration of 101s) are more frequent than those at farm (with a mean duration of 81s), because the idle at field is related to driver's turnover, attached/detached of the cutting bar, fix failures, refuel as reported by Hunt and Wilson [49]. The time contribution of the transport tasks (both on field and on road) are quite similar for the two combines, this can be explained by the fact that the transport at field includes all the moving activities such as the travel to reach the unloading site and back or the movement between the fields as shown in Figure 3.2. The time contribution of the headland turns was around 10% of the entire working time for both the combines. The headland turn contribution of the monitored combines was lower than the one reported by Doungpueng et al. [62], this is related to the fact that the mean area of the harvested fields reported by Doungpueng was around 0.5 ÷ 0.8ha, while the recorded mean field area for C1 and C2 were 4.42 and 8.42ha respectively.

Figure 3.2: Classification of the dataset points on the basis of the identified tasks.

The two combines accumulated 915,570 headland turns and the empirical cumulative distribution of headland duration is reported in Figure 3.3. This parameter ranges from 2 up to 283 seconds and it is strictly correlated to the headland patterns. The 50% of the headlands turn ranged between 2 and 20 seconds, this is probably related to the fact that most of the headland turns are performed in continuous, which means without having to manoeuvre. Headland turns comprised between 20 and 40 seconds are not infrequent, and they accounted for almost 20% of the headlands. Headland turns longer than 40 seconds are not infrequent; indeed, they are accounted for less than 7% of all headlands; these are probably related to a particular field's characteristics such as the presence of obstacles, or a particular field shape. These situations as reported by Bochtis et al.[63] and can influence in a certain way the performance of the entire harvesting activity because, in these circumstances, operators have to reduce the vehicle speed and perform different manoeuvres in order to be able to cover the field area.

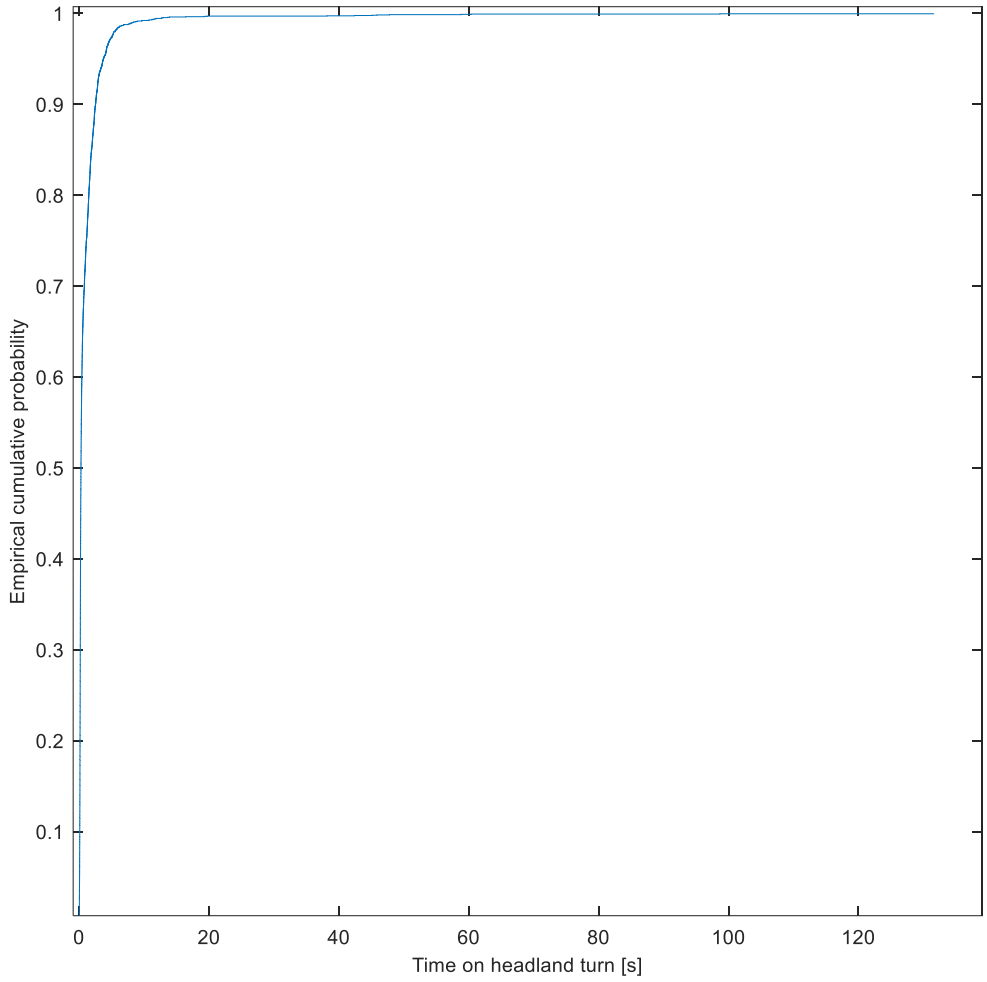

Figure 3.3: Empirical cumulative probability of the headland turns duration.

The daily usage of the combines ranges from less than 20 to up to 946 minutes; in 50% of the worked days, the combines were used for more than 350 minutes as reported in Figure 3.4.

The performance of the algorithm to perform the automated tasks identification were tested manually and visually by adding to the plot obtained after performing the automated task identification, the shapefile of the Bologna's Province roads. As shown in Figures 3.5 and 3.6, all the points were classified in one of the possible defined tasks; in particular, it was able to take a look at the perfect transitions between the transport on road and the transport on field and how smoothly the combine trajectory follows the roadway of the shapefile as shown in Figure 3.5 (a) and Figure 3.5 (b).

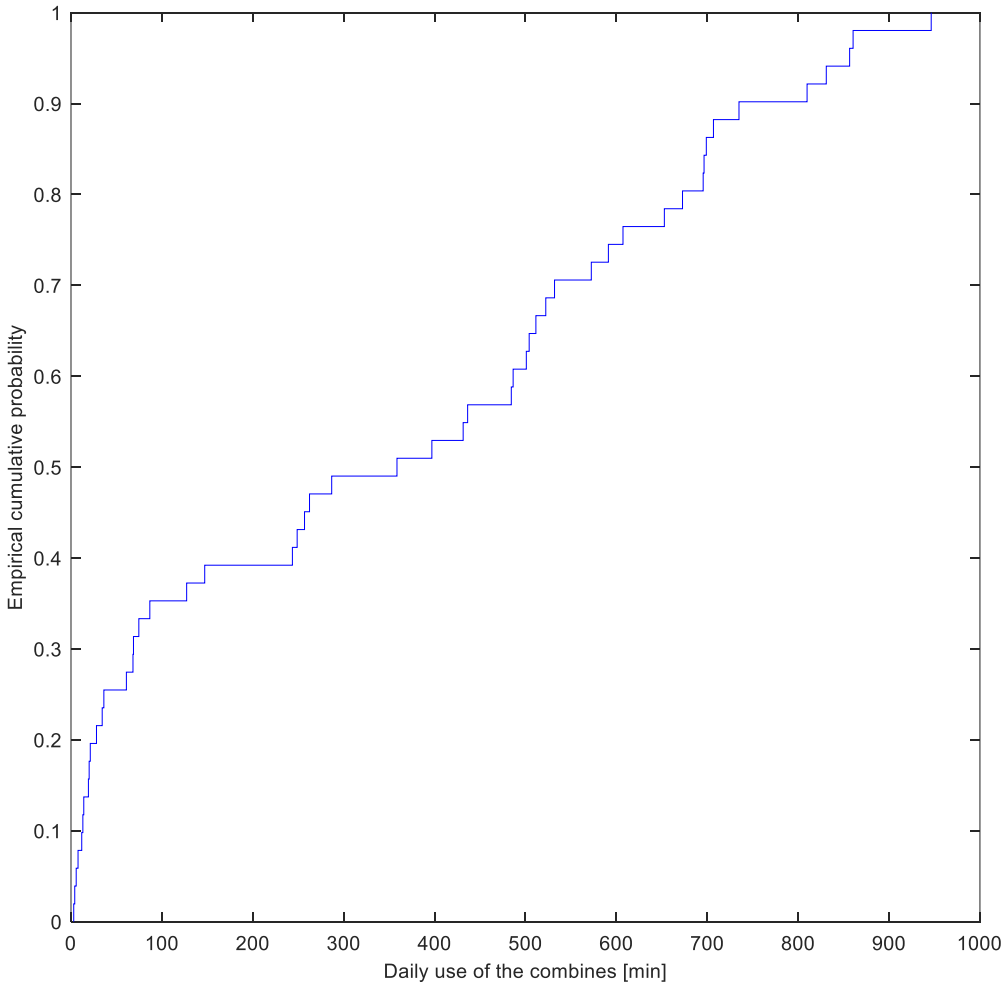

Figure 3.4: Empirical cumulative probability of the daily usage of the combine harvester

The algorithm was able to correctly classify all the points into the seven identified tasks, but not in all conditions. Indeed, in Figure 3.5a and Figure 3.6a were shown fields with particular shapes that in a certain way can lead to a difficult identification of the tasks, as well as shown in Figure 3.5b and Figure 3.6b which were considered isolated fields close to the roads. For example, in Figure 3.7, the algorithm classified the points as transport on field instead than transport on road. This occurs whenever the GNSS points were located inside the boundaries of the polygons of the land use shapefile. A few misclassifications of the transport on road occurred, and this happened whenever the speed of the combines was close to 0 km h^{-1} and the on-road points were classified inside the boundaries of the polygons of the land use shapefile used to perform the on-field classification as shown in Figure 3.8. In this case, the algorithm considers the above-mentioned points as idle on field. The same kind of misclassification occurred also for the classification of the transport on field as shown in Figure 3.8 (a) and (b). A probable misclassification sometimes occurred also during the on headland turn tasks, as shown in Figure 3.9 (a) and (b) in the black circle, because in this case the headland turn lasted more than 20 seconds and included some on work points. In

these cases, it was performed a visual inspection by using satellite images of the fields in which these errors occurred, but as shown in Figure 3.10a and Figure 3.10b, the fields did not present any particular characteristics that justified the identified manoeuvres. The reason for this misclassification could be probably related to the methodology adopted to identify the on headland turn's task because were considered only the two states identified by the sensors while probably there could be also intermediate states.

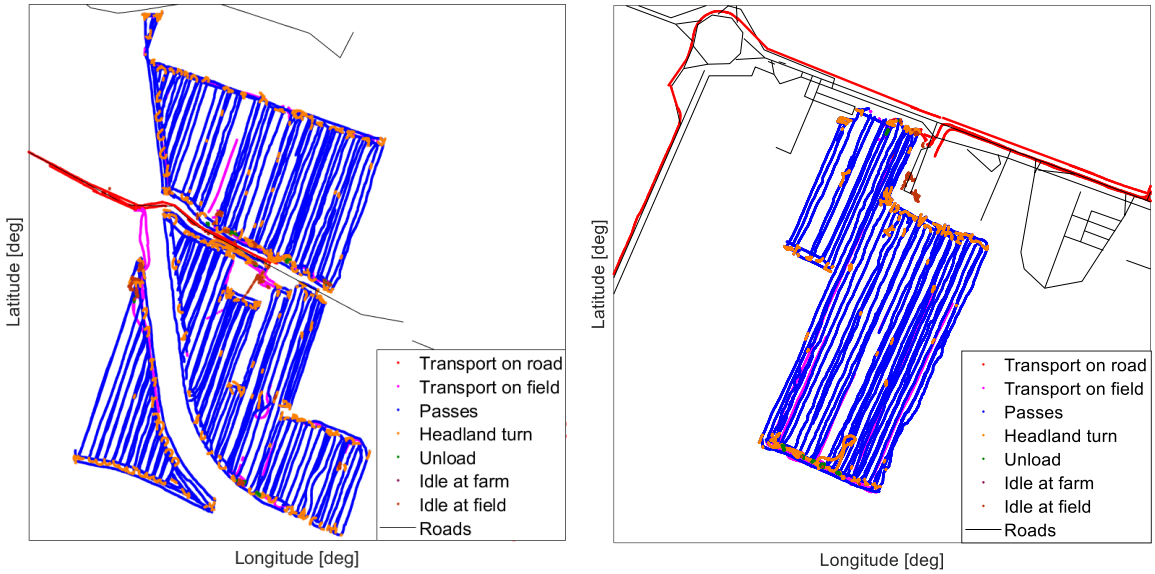

(a) *Automated task identification in fields with particular shapes*

(b) *Automated task identification in isolated fields close to the road*

Figure 3.5: Classification of the points of the dataset in the identified tasks

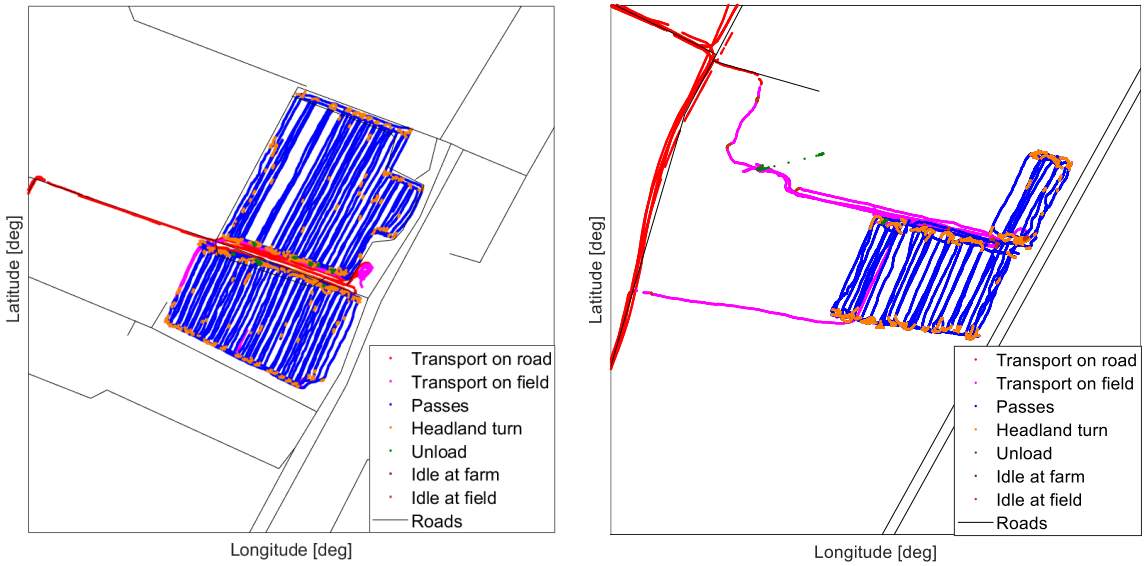

(a) *Automated task identification in fields with particular shapes*

(b) *Automated task identification in isolated fields close to the road*

Figure 3.6: Classification of the points of the dataset in the identified tasks

Figure 3.7: Examples of problems encountered after the tasks classification

.

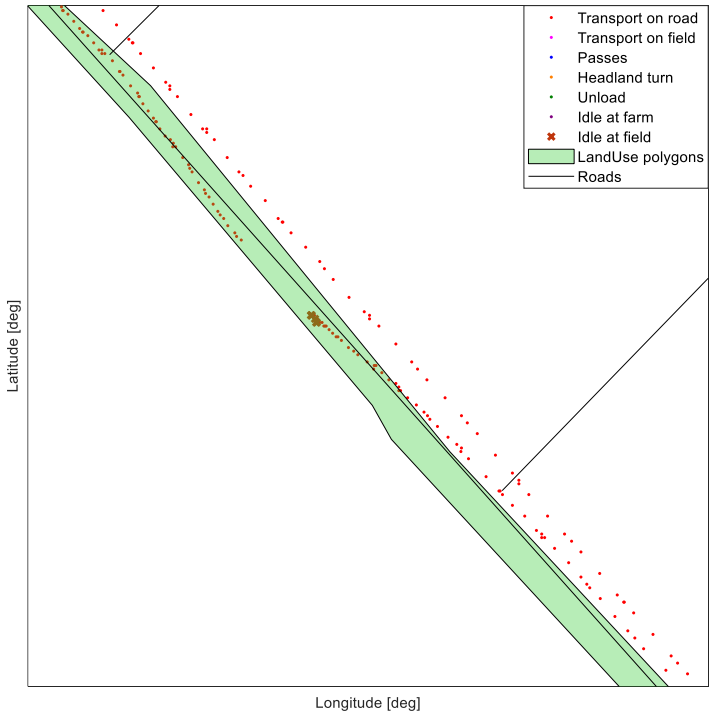

Figure 3.8: Examples of problems encountered after the tasks classification

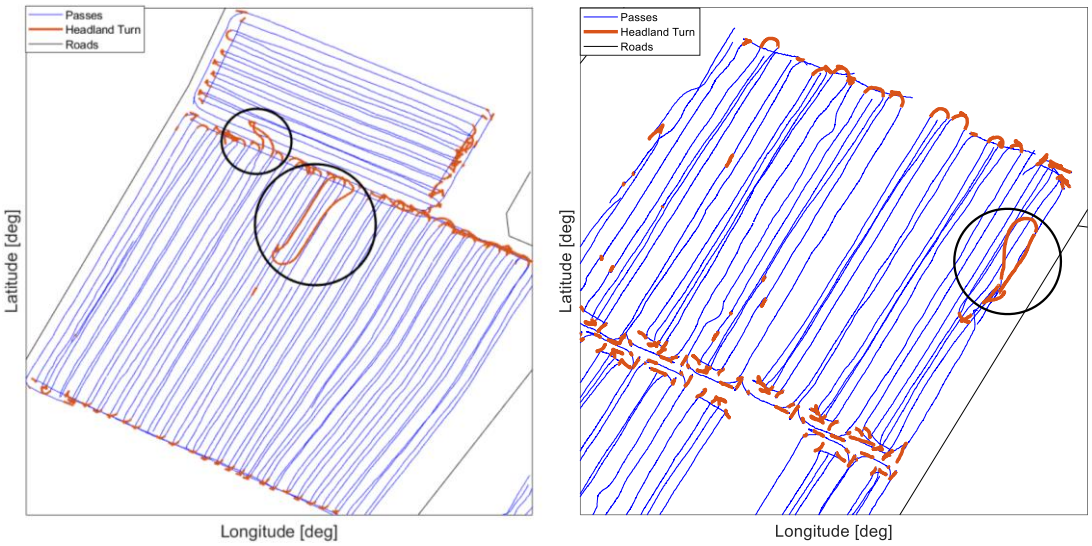

(a) The particular headland turns were highlighted in orange

(b) The particular headland turns were highlighted in orange

Figure 3.9:Identification of particular headland turn

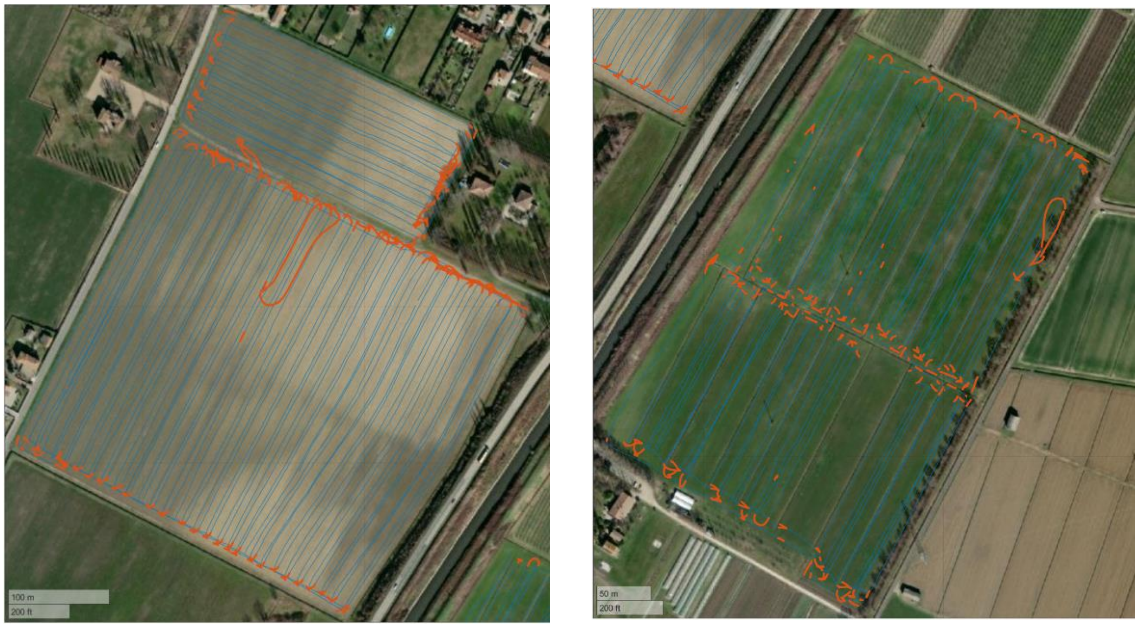

(a) Satellite image of the investigated field with a particular headland turn

(b) Satellite image of the investigated field with a particular headland turn

Figure 3.10: Satellite images for checking the reasons for the headland turn misclassification, in orange highlighted the headland turns while in blue the combine's passes

3.2 Automated fields boundaries identification

As shown in Figure 3.11, a first analysis of the results of the algorithm showed that the field clustering algorithm permitted correctly identifying most of the harvested fields but to perform a more precise performance evaluation, a visual and manual validation was carried out. For this reason, the obtained automatically identified field boundaries were checked with those manually created with QGIS. The comparison between the two, permitted it to spot possible misclassifications. As shown in Figure 3.12, Figure 3.13, Figure 3.14, and Figure 3.15, Figure 3.16 and Figure 3.17, there were reported different and particular cases

in which the automated field boundaries identification was tested. In Figures 3.12 and 3.15 there were tested fields with a simple shape and orthogonal field boundaries, in which the identified boundaries were similar to the boundaries identified manually. In Figures 3.13, Figure 3.14 and Figure 3.16 there were tested fields with particular shapes and a hole inside, in these cases the identified boundaries were in few parts not following the manually identified boundaries. Figure 3.17 it was tested the capability of the algorithm to identify a group of fields close one to the others, the distance between the field was very small and the algorithm was not able to correctly identify the boundaries of the field. Figure 3.17 presents fields with particular shapes in which the field boundaries were irregular and the fields were not convex, in this case, the algorithm was able to correctly identify only one of the three fields. This misclassification problem could be probably related to a limit of the DBSCAN solution. Indeed, in fields that presented within them a certain reduction of the GNSS points density, the algorithm identified these areas as the edge of the fields and clustered them as different fields.

One can note that in the case of fields with a distance among the headlands lower than 6 m the misclassification occurred as shown in Figure 3.20.

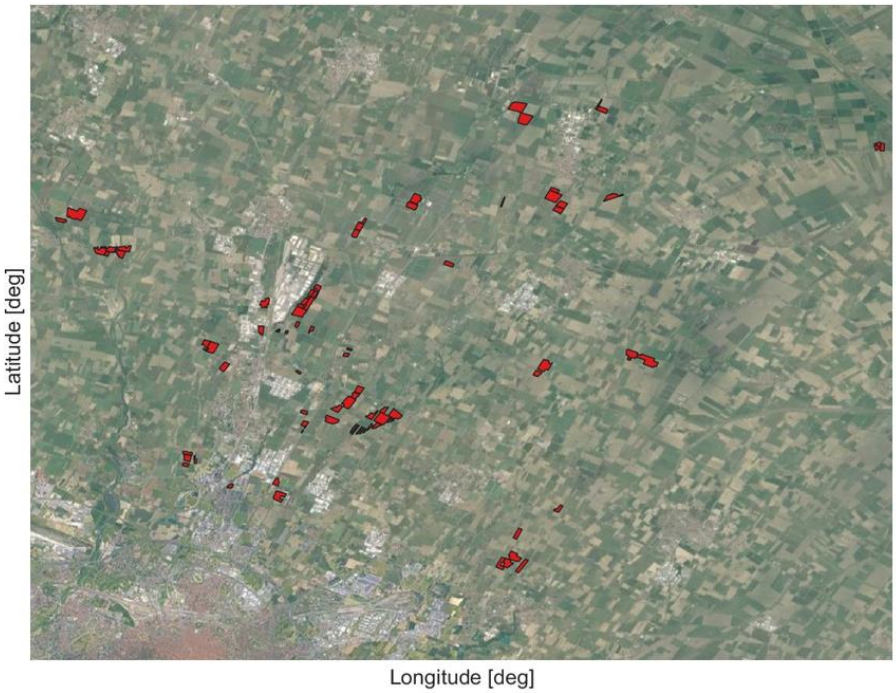

Figure 3.11: Field identification performed by the algorithm, the GNSS points of the combine harvester were clustered by using the "DBSCAN" function

Figure 3.12: Visual check of the capability of the algorithm to automatically identify the field boundaries in isolated fields

Figure 3.13: Visual check of the capability of the algorithm to automatically identify the field boundaries in fields isolated with a particular shape

Figure 3.14: Visual check of the capability of the algorithm to automatically identify the field boundaries in fields with particular shapes and holes inside.

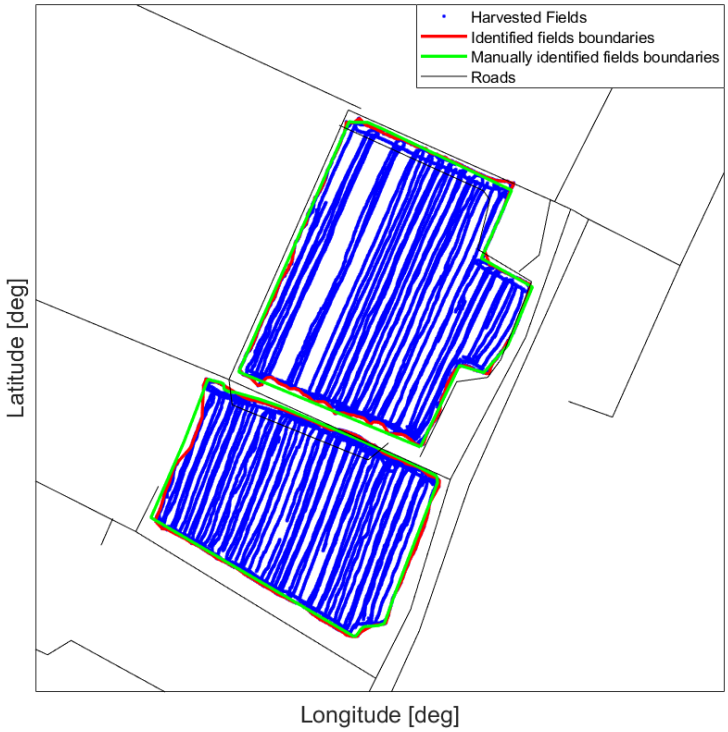

Figure 3.15: Visual check of the capability of the algorithm to automatically identify the field boundaries in fields with long distances between the headlands

Figure 3.16: Visually check the capability of the algorithm to automatically identify the field boundaries in fields with different shape

Figure 3.17: Visually check the capability of the algorithm to automatically identify the field boundaries in fields with different distance

In Figure 3.18 there were reported two fields very close one to the other, in which the harvesting pattern in the two fields were orthogonal. In this case, the algorithm was not able

to correctly identify the field boundaries. The field shown in Figure 3.19 presents a very particular shape and a low harvesting pattern. As a low harvesting pattern, it was considered the presence of a great number of parts inside the field in which the combines had not performed harvesting. In this case, the algorithm was able to correctly identify the field boundaries. Figure 3.20 were shown two fields in which in the first the distance between the headlands was lower than 6m and in the latter, the distance was greater than 6m. In the first case, the algorithm was not able to correctly identify the boundaries of the two fields while in the latter th automated identification worked properly.

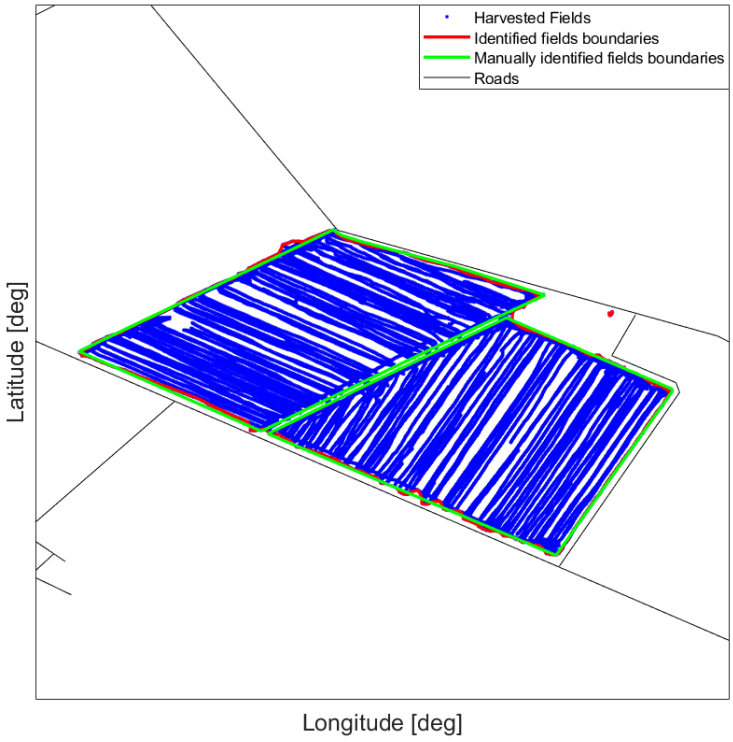

Figure 3.18: Visually check of the capability of the algorithm to automatically identify the field boundaries in fields very close to each other

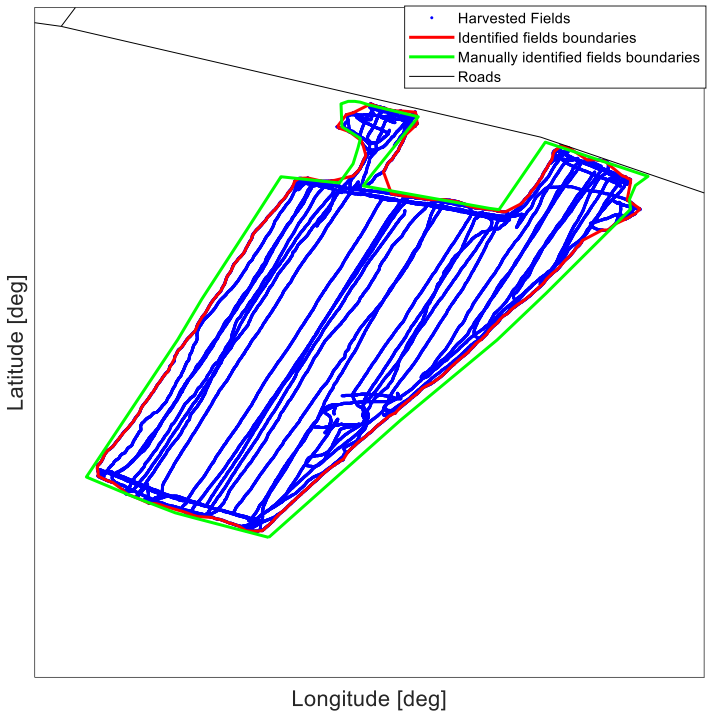

Figure 3.19: Visually check the capability of the algorithm to automatically identify the field boundaries of fields with particular shapes

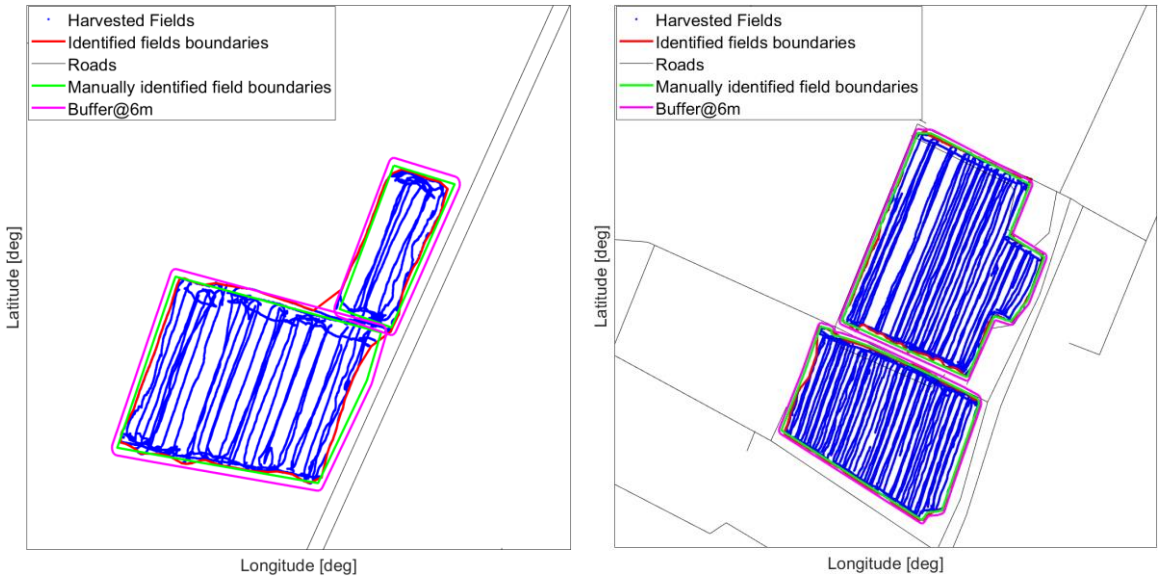

(a) Headland distance lower than 6 m *(b) Headland distance higher than 6m*

Figure 3.20: Identification of the threshold headland distance that introduces misclassification

However, the algorithm identified the field's boundaries of 39 harvested fields instead of 54 fields harvested in 2020; while in 2022 the identified field's boundaries were 72 instead of 96 harvested fields. In addition, the identified field boundaries follow strictly, in most cases, the line of the real field boundaries as shown in Figure 3.12 and Figure 3.15.

3.3 Combine harvesters performance evaluation

During harvesting season 2020, the combines have harvested a total of 54 fields and over an area of 461 ha as shown in Figure 3.20, while during 2022 the combines have harvested a total of 96 fields and over an area of 420 ha as shown in Figure 3.21. In 2020, C1 and C2 harvested 184 and 277 ha, respectively; while, in 2022, C1 and C2 harvested 200 and 219 ha, respectively (Table 3.1).

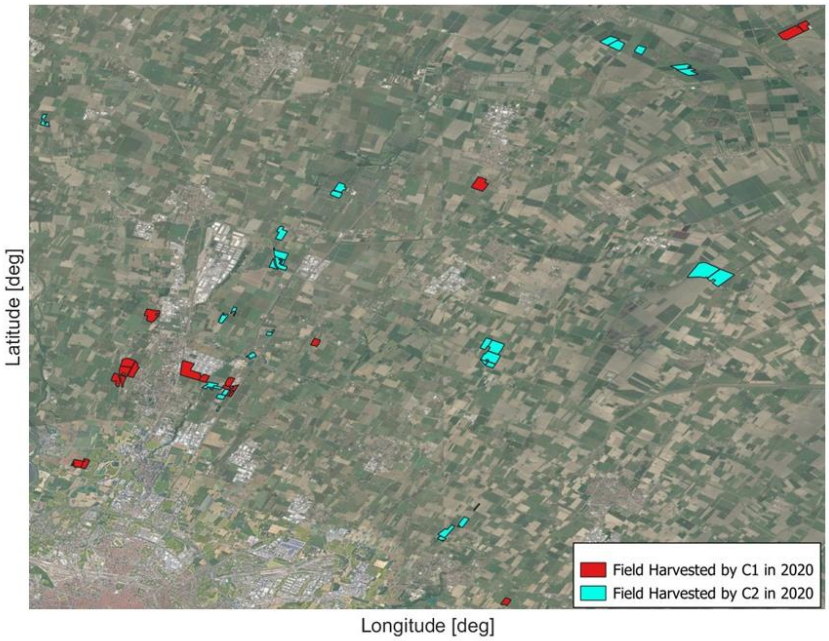

Figure 3.21: Fields harvested by each one of the combines in 2020

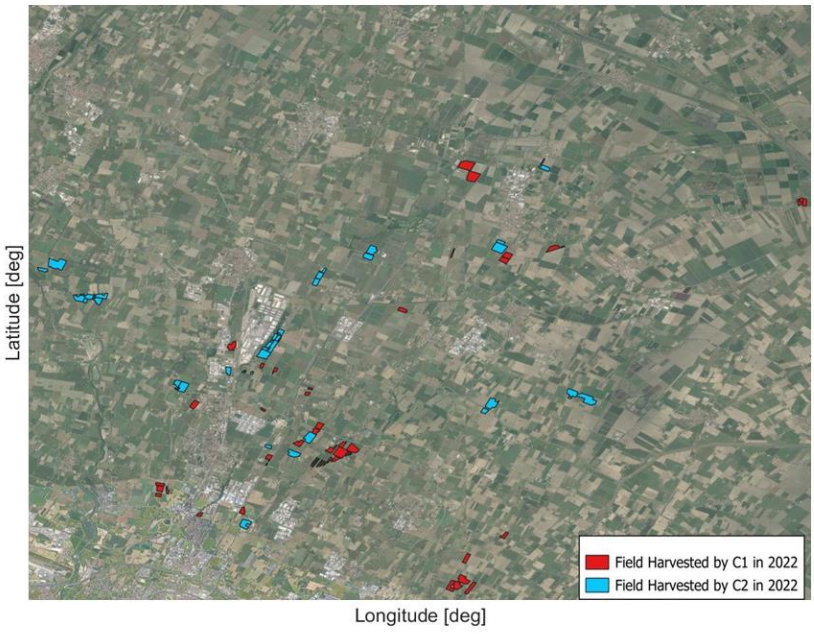

Figure 3.22: Fields harvested by each one of the combines in 2022

The increase in the number of harvested fields in 2022 compared to the number of fields harvested in 2020 is related to the fact that as discovered during the development of the shapefile in which field boundaries were manually reported, the mean field area in 2020 and 2022 were 5.23 and 3.78 ha respectively. This implies a mean area reduction of almost 28%.

Table 3.1: Summary table of the data obtained by the performed analysis for the harvesting seasons 2020 and 2022

	C1	C2
Passes (%)	68.00 %	62.00 %
Headland turn (%)	13.00 %	10.00 %
Idle at field (%)	10.00 %	13.00 %
Idle at farm (%)	0.92 %	2.00 %
Transport at road (%)	4.00 %	5.00 %
Transport at field (%)	3.00 %	5.00 %
Unload (%)	<1.00 %	2.00 %
Harvested area (ha)	384.17	498.69
Total fuel consumption (L)	9,871.20	11,011.90
Fuel consumption on road (%)	5.50 %	6.00 %
Fuel consumption on field (%)	94.50 %	94.00 %

In Table 3.1, C1 and C2 present similar values of field annual working time, which comprise passes and headland turn, high effective working time that comprises only the passes and lower harvested area than the data presented in another study [64]. The lower value of the harvested area is probably related to the unique orographic characteristics of the Italian peninsula. Indeed, Italy presents a limited amount of arable land, 41% of the entire Italian surface [65], and this amount results fragmented in small fields due to the historical and land use planning policies such as sharecropping and the creation of the cadastre. In addition, in each Italian province, there are several agricultural contractors that share out the managed arable land. This implies that the annual harvested area performed by the monitored combines results lower than the area reported by Olt et al [64]. The data of the fuel consumption result similar to that presented by Olt et al. [64] for C1 while resulted higher in C2; by considering the fuel consumption on road operations, the values result higher, while the fuel consumption on field resulted lower than the values presented in the literature [64]. The fuel consumption on road result higher due to the distance between the farm site and the harvested fields, indeed they were spread over an area of almost 445 km^2 around the farm site. This certainly determined the increase of the fuel consumption on road and the reduction

of the fuel consumption on field of the monitored combines. The measured parameters for the monitored combines resulted lower than in most of the computed values reported in Table 3.2.

Table 3.2: Agro-technical characteristics of the monitored combines

	C1	C2
Harvested weight performance (t h^{-1})	11.35 (5.87)	8.87 (2.90)
Harvesting performance (t ha^{-1})	7.14 (3.26)	5.72 (1.72
Total harvested crops (t)	2,744.36 (47.51)	2,852.86 (52.12)
Field capacity (ha h^{-1})	1.59 (0.48)	1.90 (0.16)
Total fuel consumption per hour (L h^{-1})	40.82 (2.33)	41.88 (3.02)
Fuel consumption per area (L ha^{-1})	25.69 (5.41)	22.08 (2.98)
Fuel consumption per total harvested crops (L t^{-1})	3.60 (1.07)	3.86 (0.54)

These values can be probably related to the yield of the harvested crops and to the field's shape as reported by Bochtis et al [63]. By comparing the field capacity of the monitored combines it was found that the values were similar to the value reported by Latterini et al. [66]. Instead, the values of the fuel consumption resulted higher than the values reported by Olt et al. [64], this is probably related as above mentioned to the field's shape that determines an increase of the time in harvesting and consequently an increase of the fuel consumption.
As noted in Table 3.3 and also in Table 3.4, there were considered the mean power and speed values for each task. The value of the speed for the idles and unload task was intentionally omitted due to the fact that one of the rules for the identification of these tasks was that combines had to be standstill.
By considering Table 3.3 the lowest $\bar{P}_{eng}$ values were found during idling conditions, at farm and at field, the values recorded during the transport tasks were lower than 100 kW and this value is lower than that occurring at on passes and unloading activities. This can be related to the fact that the power required was used only for moving the machines. For on passes and unload tasks, the power was required to activate other combine components such as the cutting bar, threshing system, and cleaning system during harvesting. On the other hand, during unloading was mandatory to activate the unloading system, composed of an auger. During the transport on road, $\bar{V}$ resulted higher than that during transport on field, this relation between the different speeds on road and on field was explained also by Zhang et al [44]. Speed lower than 4 km h^{-1} during on work task was related to the crop yield and to the field's shape as reported by Bochtis et al [63] and as found out by the presence of obstacles on field as shown in Figure 3.22 that require a temporary speed slowing down.

Table 3.3: Power demands per each task

$\bar{P}_{eng}$ $[kW]$	C1	C2
Idle at farm	13.04 (12.20)	13.94 (10.78)
Idle at field	12.80 (8.89)	13.64 (9.71)
Transport on road	84.37 (50.77)	95.88 (50.65)
Transport on field	91.73 (64.89)	94.30 (54.80)
On work	168.08 (35.84)	168.74 (38.26)
Unload	114.06 (37.79)	108.14 (33.87)
Total	134.34 (70.76)	130.80 (68.61)

Table 3.4: Mean speed detected per each task

$\bar{V}$ $[km\ h^{-1}]$	C1	C2
Transport on road	25.78 (12.26)	27.79 (11.33)
Transport on field	7.73 (5.46)	6.95 (5.17)
On work	3.91 (2.18)	3.96 (1.95)
Total	4.69 (6.52)	4.87 (7.04)

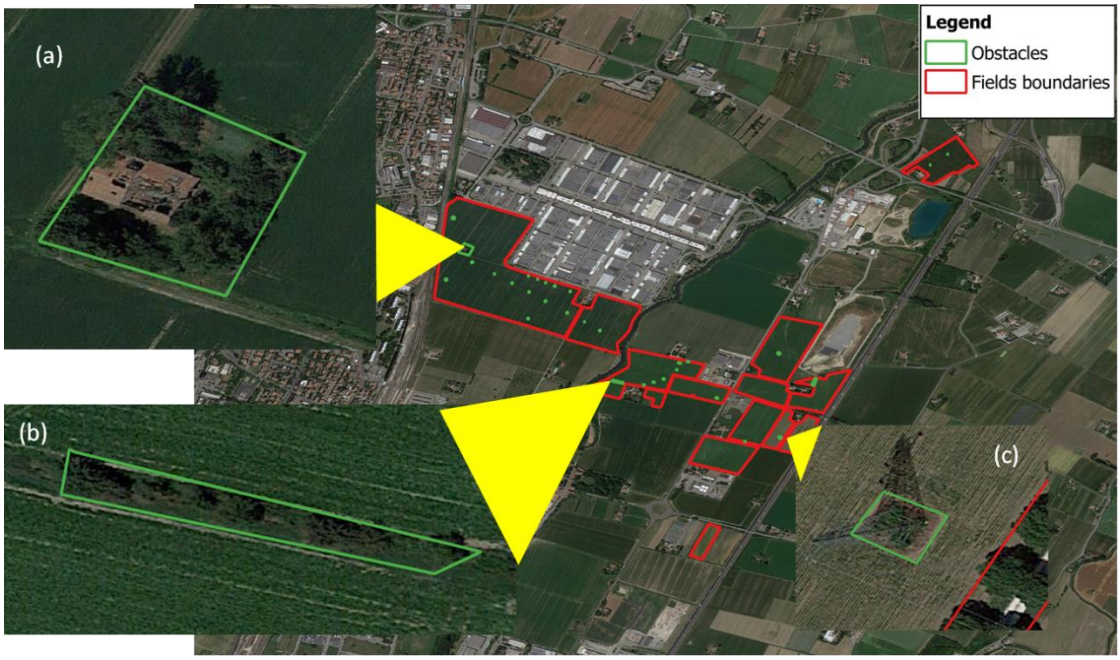

Figure 3.23: Visual identification of obstacles on field that could reduce the speed during on work task. (a) the presence of old rural buildings, (b) wooded strips, (c) Power lines

The Spearman correlation matrix was obtained with the measured data from the combines performance and the harvested fields. Figure 3.23, shown a negative and positive strong correlation between the parameters referred to the field characteristics such as A, P and F_{sr}.

A	1.00								
P	0.91	1.00							
F_{sr}	-0.89	-0.67	1.00						
t	0.98	0.89	-0.89	1.00					
F_c	0.52	0.51	-0.43	0.40	1.00				
F_{consH}	0.96	0.87	-0.86	0.97	0.38	1.00			
C_{YH}	-0.10	-0.11	0.09	-0.07	-0.25	0.08	1.00		
$\bar{V}$	0.23	0.22	-0.19	0.22	0.08	0.21	-0.03	1.00	
$\bar{P}_{eng}$	-0.24	-0.23	0.21	-0.25	-0.11	-0.04	0.73	-0.15	1.00
	A	P	F_{sr}	t	F_c	F_{consH}	C_{YH}	$\bar{V}$	$\bar{P}_{eng}$

Figure 3.24:Results of Spearman's correlation matrix. High positive correlations are highlighted in dark green, and high negative correlations are in dark red

While the parameters that considered the combine's performance (i.e. F_c, C_{YH}, F_{consH}, $\bar{P}_{eng}$ and $\bar{V}$) and present positive and negative weak correlations with the field's characteristics, except the $\bar{P}_{eng}$ that presented a strong positive correlation with the C_{YH}. This is probably related to the fact that as reported by Bochtis et al. [63], the characteristics of the crops such as the crop density or the obtained yield could influence the operational parameters of the agricultural machinery. Indeed, the engine power during on work is influenced by crop density since there is a greater amount of crop that must be threshed and cleaned.

Chapter 4

4 Conclusions

The main goal of this study was to investigate in which and how many activities the combined harvesters were involved, as well as how much time they spent in each activity. Thus, two combine harvesters were monitored for two years in real-world conditions. In addition, it was developed a methodology to perform an automated identification of field boundaries and a performance evaluation for each single field. The proposed methodology was able to identify all the tasks in which the combines were involved, during harvesting season, and the observed values are similar to the values presented in the literature. In addition, the algorithm was able to correctly identify most of the harvested fields. The adoption of the DBSCAN and of the alphashape to perform the automated field boundaries identification was helpful to obtain information about the characteristics of the harvested fields. However, in fields with irregular boundaries, the algorithm struggled to identify the right boundaries. Moreover, the clustering algorithm struggles in discerning fields that are very close to each other. It was also observed a certain difficulty to compare the data for the monitored combines with data present in the literature. Indeed, the values observed for the monitored combines result lower, in particular the values of the total working time and of the total harvested area. Those problems could be related to the Italian agricultural situation, which results quite different than that of other countries, due to the fact that the arable land represents only 41% of the whole territory.

By considering the performance parameters observed for the two monitored combines also in this situation the values resulted lower than the values found in the literature. This is probably related to the different characteristics of the harvested fields such as the parameters of the fields shape ratio resulted quite differently, sometimes the presence of different kinds of obstacles that required a certain skill from the operators to reduce the number of slowing down during harvesting that otherwise inevitably reduced the harvesting performance.

In literature, similar analyses were performed abroad, but in Italy, this kind of analysis was performed only on tractors. This could be related to the fact that tractors were used for longer times during growing seasons than combine harvesters that can be used only to perform a particular operation. Indeed, in order to be able to increase the efficiency of the whole

agricultural system is mandatory primarily for manufacturers, but also for farmers and agricultural contractors, to increase the efficiency of the different subsystems related to the crops growing. Nowadays Italian farmers were facing an important transition from the old way of doing agriculture to the smart agriculture. The Italian Ministry of Agriculture thanks to the tax credit manoeuvre, called "Agricoltura 4.0", opens the possibility to renew agricultural fleets and adopt digital solutions for farmers and agricultural contractors.

The change of the old agricultural fleets with the new ones could allow obtaining more data from agricultural machinery and can increase the adoption of the proposed methodology.

Thanks to the information obtained by the model it is also possible to cover a large part of the data required by national governmental organisations, or it can be delivered to agronomists or clients who managing the farm in order to provide them a whole picture of the farm situation. The proposed methodology opens up further development of the developed algorithm, in particular on the automated field boundaries identification that needs to be more adherent to the Italian situation.

5 Bibliography

1. Sørensen, C. Workability and Machinery Sizing for Combine Harvesting. *Agricultural Engineering International : The CIGR e-journal* **2003**.
2. Miu, P. : *: Theory, Modeling, and Design*; CRC Press: Boca Raton, 2015; ISBN 978-0-429-15293-1.
3. Federico, G.; Malanima, P. Progress, Decline, Growth: Product and Productivity in Italian Agriculture, 1000–2000. *The Economic History Review* **2004**, *57*, 437–464, doi:10.1111/j.1468-0289.2004.00284.x.
4. Keicher, R.; Seufert, H. Automatic Guidance for Agricultural Vehicles in Europe. *Computers and Electronics in Agriculture* **2000**, *25*, 169–194, doi:10.1016/S0168-1699(99)00062-9.
5. Perez-Ruiz, M.; K., S. GNSS in Precision Agricultural Operations. In *New Approach of Indoor and Outdoor Localization Systems*; Elbahhar, F., Ed.; InTech, 2012 ISBN 978-953-51-0775-0.
6. Lips, M.; Burose, F. Repair and Maintenance Costs for Agricultural Machines. *International Journal of Agricultural Management* **2012**, *1*, 7.
7. Mimra, M.; Kavka, M. Risk Analysis Regarding a Minimum Annual Utilization of Combine Harvesters in Agricultural Companies. **2017**, 469.4Kb, doi:10.15159/AR.17.022.
8. Calcante, A.; Fontanini, L.; Mazzetto, F. Repair and Maintenance Costs of 4WD Tractors and Self Propelled Combine Harvesters in Italy. *J Agricult Engineer* **2013**, *44*, doi:10.4081/jae.2013.312.
9. The Analysis of the Operating Conditions of Farm Machinery Engines in Regard to Exhaust Emissions Legislation. *Appl. Eng. Agric.* **2013**, doi:10.13031/aea.29.9833.
10. Botta, G.F.; Tolón-Becerra, A.; Bienvenido, F.; Rivero, E.R.D.; Andrés, D.; Contessotto, E.E.; Fonterosa, R.A.; Agnes, D.W. Traffic of Harvester Combines: Effect on Maize Yields (Zea Mays L.) and Soil Compaction under Direct Sowing System. *Revista de la Facultad de Ciencias Agrarias. Universidad Nacional de Cuyo* **2018**, *50*, 85–100.
11. Lamandé, M.; Greve, M.H.; Schjønning, P. Risk Assessment of Soil Compaction in Europe – Rubber Tracks or Wheels on Machinery. *CATENA* **2018**, *167*, 353–362, doi:10.1016/j.catena.2018.05.015.
12. Søgaard, H.T.; Sørensen, C.G. A Model for Optimal Selection of Machinery Sizes within the Farm Machinery System. *Biosystems Engineering* **2004**, *89*, 13–28, doi:10.1016/j.biosystemseng.2004.05.004.
13. Sørensen, C.G.; Bochtis, D.D. Conceptual Model of Fleet Management in Agriculture. *Biosystems Engineering* **2010**, *105*, 41–50, doi:10.1016/j.biosystemseng.2009.09.009.
14. Auernhammer, H. Precision Farming — the Environmental Challenge. *Computers and Electronics in Agriculture* **2001**, *30*, 31–43, doi:10.1016/S0168-1699(00)00153-8.
15. Wang, Y.-J.; Huang, G.Q. Harvester Scheduling Joint with Operator Assignment. *Computers and Electronics in Agriculture* **2022**, *202*, 107354, doi:10.1016/j.compag.2022.107354.
16. Böttinger, S.; Fliege, L. Working Performance of Cleaning Units of Combine Harvesters on Sloped Fields. **2012**, Landtechnik *67*, 34–36.
17. Young, S. Electronic Control System for GENESIS™ 70 Series Tractors. *SAE Transactions* **1994**, *103*, 243–251.
18. Molari, G.; Mattetti, M.; Perozzi, D.; Sereni, E. Monitoring of the Tractor Working Parameters from the CAN-Bus. *Journal of Agricultural Engineering* **2013**, *44*, doi:10.4081/jae.2013.319.
19. Mattetti, M.; Maraldi, M.; Lenzini, N.; Fiorati, S.; Sereni, E.; Molari, G. Outlining the Mission Profile of Agricultural Tractors through CAN-BUS Data Analytics. *Computers and Electronics in Agriculture* **2021**, *184*, 106078, doi:10.1016/j.compag.2021.106078.
20. Liew, C.T. Development of Tractor Instrumentation System: Hydraulics, and Controller Area Network (CAN) Data Analysis of Agricultural Machinery. 136.
21. Salim, F.; Darr, M.; Covington, B.; Powell, L. *The Performance of Farm Tractors as Reported by CAN-BUS Messages*; 2016;
22. Ludes, R.; Steeples, B. *Road Load and Customer Data from the Vehicle Data Bus - A New Approach for Quality Improvement*; SAE International: Warrendale, PA, 1999;
23. Molari, G.; Mattetti, M.; Lenzini, N.; Fiorati, S. An Updated Methodology to Analyse the Idling of Agricultural Tractors. *Biosystems Engineering* **2019**, *187*, 160–170, doi:10.1016/j.biosystemseng.2019.09.001.

24. Webster, R.T. *Statistical Methods in Soil and Land Resource Survey / R. Webster and M. A. Oliver*; Spatial information systems; University press: Oxford, 1990; ISBN 0-19-823316-7.
25. Wolf, S.A. *Privatization of Information and Agricultural Industrialization*; CRC Press, 1997; ISBN 1-57444-104-3.
26. Tomer, M.D.; James, D.E.; Sandoval-Green, C.M.J. Agricultural Conservation Planning Framework: 3. Land Use and Field Boundary Database Development and Structure. *Journal of Environmental Quality* **2017**, *46*, 676–686, doi:10.2134/jeq2016.09.0363.
27. Marvaniya, S.; Devi, U.; Hazra, J.; Mujumdar, S.; Gupta, N. Small, Sparse, but Substantial: Techniques for Segmenting Small Agricultural Fields Using Sparse Ground Data. *International Journal of Remote Sensing* **2021**, *42*, 1512–1534, doi:10.1080/01431161.2020.1834166.
28. Buchhorn, M.; Lesiv, M.; Tsendbazar, N.E.; Smets, B.; Bertels, L.; Van De Kerchove, R.; Herold, M.; Masiliunas, D.; Fritz, S. Copernicus Global Land Cover Service - Elastic, Operational Land Cover Mapping at Global Scale Using Time Series Analysis. **2019**, *2019*, B23C-02.
29. Canny, J. A Computational Approach to Edge Detection. *IEEE Transactions on Pattern Analysis and Machine Intelligence* **1986**, *PAMI-8*, 679–698, doi:10.1109/TPAMI.1986.4767851.
30. Kocur-Bera, K. Data Compatibility between the Land and Building Cadaster (LBC) and the Land Parcel Identification System (LPIS) in the Context of Area-Based Payments: A Case Study in the Polish Region of Warmia and Mazury. *Land Use Policy* **2019**, *80*, 370–379, doi:10.1016/j.landusepol.2018.09.024.
31. Taşdemir, K.; Wirnhardt, C. Neural Network-Based Clustering for Agriculture Management. *EURASIP J. Adv. Signal Process.* **2012**, *2012*, 200, doi:10.1186/1687-6180-2012-200.
32. Matikainen, L.; Karila, K.; Litkey, P.; Ahokas, E.; Munck, A.; Karjalainen, M.; Hyyppä, J. The challenge of automated change detection: Developing a method for the updating of land parcels. *ISPRS Ann. Photogramm. Remote Sens. Spatial Inf. Sci.* **2012**, *I–4*, 239–244, doi:10.5194/isprsannals-I-4-239-2012.
33. Sonobe, R.; Yamaya, Y.; Tani, H.; Wang, X.; Kobayashi, N.; Mochizuki, K. Crop Classification from Sentinel-2-Derived Vegetation Indices Using Ensemble Learning. *JARS* **2018**, *12*, 026019, doi:10.1117/1.JRS.12.026019.
34. Sentinel-2 Cropland Mapping Using Pixel-Based and Object-Based Time-Weighted Dynamic Time Warping Analysis | Elsevier Enhanced Reader Available online: https://reader.elsevier.com/reader/sd/pii/S0034425717304686?token=7EB94788AC3349CF736C6D7998336523C10874390F911E90A939044D7314A557F940965B9860EC5003F696E892D2664D&originRegion=eu-west-1&originCreation=20221201080023 (accessed on 1 December 2022).
35. Lebourgeois, V.; Dupuy, S.; Vintrou, É.; Ameline, M.; Butler, S.; Bégué, A. A Combined Random Forest and OBIA Classification Scheme for Mapping Smallholder Agriculture at Different Nomenclature Levels Using Multisource Data (Simulated Sentinel-2 Time Series, VHRS and DEM). *Remote Sensing* **2017**, *9*, 259, doi:10.3390/rs9030259.
36. Masoud, K.M.; Persello, C.; Tolpekin, V.A. Delineation of Agricultural Field Boundaries from Sentinel-2 Images Using a Novel Super-Resolution Contour Detector Based on Fully Convolutional Networks. *Remote Sensing* **2020**, *12*, 59, doi:10.3390/rs12010059.
37. Chen, Y.; Li, G.; Zhang, X.; Jia, J.; Zhou, K.; Wu, C. Identifying Field and Road Modes of Agricultural Machinery Based on GNSS Recordings: A Graph Convolutional Neural Network Approach. *Computers and Electronics in Agriculture* **2022**, *198*, 107082, doi:10.1016/j.compag.2022.107082.
38. Marketos, G.; Frentzos, E.; Ntoutsi, I.; Pelekis, N.; Raffaetà, A.; Theodoridis, Y. Building Real-World Trajectory Warehouses. In Proceedings of the Proceedings of the Seventh ACM International Workshop on Data Engineering for Wireless and Mobile Access; Association for Computing Machinery: New York, NY, USA, June 13 2008; pp. 8–15.
39. Zheng, Y. Trajectory Data Mining: An Overview. *ACM Trans. Intell. Syst. Technol.* **2015**, *6*, 29:1-29:41, doi:10.1145/2743025.
40. Schuessler, N.; Axhausen, K.W. Processing Raw Data from Global Positioning Systems without Additional Information. *Transportation Research Record* **2009**, *2105*, 28–36, doi:10.3141/2105-04.
41. Ester, M.; Kriegel, H.-P.; Sander, J.; Xu, X. A Density-Based Algorithm for Discovering Clusters in Large Spatial Databases with Noise.

42. Zhang, X.; Chen, Y.; Jia, J.; Kuang, K.; Lan, Y.; Wu, C. Multi-View Density-Based Field-Road Classification for Agricultural Machinery: DBSCAN and Object Detection. *Computers and Electronics in Agriculture* **2022**, *200*, 107263, doi:10.1016/j.compag.2022.107263.
43. Davies, D.L.; Bouldin, D.W. A Cluster Separation Measure. *IEEE Transactions on Pattern Analysis and Machine Intelligence* **1979**, *PAMI-1*, 224–227, doi:10.1109/TPAMI.1979.4766909.
44. Zhang, Y.; Balmos, A.; Krogmeier, J.V.; Buckmaster, D. Working Zone Identification for Specialized Micro Transportation Systems Using GPS Tracks. In Proceedings of the 2015 IEEE 18th International Conference on Intelligent Transportation Systems; September 2015; pp. 1779–1784.
45. Buchanan, B.G.; Duda, R.O. Principles of Rule-Based Expert Systems. In *Advances in Computers*; Yovits, M.C., Ed.; Advances In Computers; Elsevier, 1983; Vol. 22, pp. 163–216.
46. Edelsbrunner, H.; Kirkpatrick, D.; Seidel, R. On the Shape of a Set of Points in the Plane. *IEEE Transactions on Information Theory* **1983**, *29*, 551–559, doi:10.1109/TIT.1983.1056714.
47. Layton, A.W.; Zhang, Y.; Krogmeier, J.V.; Buckmaster, D.R. <I>Determining Harvesting Efficiency via Multiple Combine GPS Logs</I> In Proceedings of the 2017 Spokane, Washington July 16 - July 19, 2017; American Society of Agricultural and Biological Engineers, 2017.
48. Bochtis, D.D.; Sørensen, C.G.; Vougioukas, S.G. Design and Modelling Approaches for Advanced Agricultural Fleet Management Systems Available online: https://www.igi-global.com/chapter/design-modelling-approaches-advanced-agricultural/www.igi-global.com/chapter/design-modelling-approaches-advanced-agricultural/54406 (accessed on 21 September 2022).
49. Hunt, D.; Wilson, D. *Farm Power and Machinery Management: Eleventh Edition*; Waveland Press, 2015; ISBN 978-1-4786-3177-4.
50. Grisso, R.; Jasa, P.; Rolofson, D. Analysis of Traffic Patterns and Yield Monitor Data for Field Efficiency Determination. *Applied Engineering in Agriculture* **2002**, *18*, 171–178, doi:10.13031/2013.7782.
51. Pitla, S.; Lin, N.; Shearer, S.; Luck, J. Use Of Controller Area Network (Can) Data To Determine Field Efficiencies Of Agricultural Machinery. *Applied engineering in agriculture* **2015**, *30*, 829–839, doi:10.13031/aea.30.10618.
52. Zhou, K.; Bochtis, D.; Jensen, A.L.; Kateris, D.; Sørensen, C.G. Introduction of a New Index of Field Operations Efficiency. *Applied Sciences* **2020**, *10*, 329, doi:10.3390/app10010329.
53. SAE *J1939/14_202204: Physical Layer, 500 Kbit/s - (SAE J1939-14; Pagg. 1–13).*;
54. SAE *J1939/15_201812: Physical Layer, 250 Kbps - (SAE J1939-15; Pagg. 1–20)*;
55. Camshaft and Crankshaft Sensors Available online: https://www.denso-am.eu/products/engine-management-systems/camshaft-crankshaft-sensors (accessed on 7 March 2023).
56. *Tractors and Machinery for Agriculture and Forestry. Serial Control and Communications Data Network General Standard for Mobile Data Communication*; Confirmed.; 2018; ISBN 978-0-580-74597-3.
57. Heiß, A.; Paraforos, D.; Griepentrog, H. Determination of Cultivated Area, Field Boundary and Overlapping for A Plowing Operation Using ISO 11783 Communication and D-GNSS Position Data. *Agriculture* **2019**, *9*, 38, doi:10.3390/agriculture9020038.
58. Dati Preconfezionati Available online: https://geoportale.regione.emilia-romagna.it/download/dati-e-prodotti-cartografici-preconfezionati/pianificazione-e-catasto/uso-del-suolo/2017-coperture-vettoriali-uso-del-suolo-di-dettaglio-edizione-2020/dati-preconfezionati (accessed on 9 October 2022).
59. Paraforos, D.S.; Hübner, R.; Griepentrog, H.W. Automatic Determination of Headland Turning from Auto-Steering Position Data for Minimising the Infield Non-Working Time. *Computers and Electronics in Agriculture* **2018**, *152*, 393–400, doi:10.1016/j.compag.2018.07.035.
60. Witney, B. *Choosing and Using Farm Machines.*; Longman: London, 1988; ISBN 978-0-582-45600-6.
61. Savickas, D.; Steponavičius, D.; Kliopova, I.; Saldukaitė, L. Combine Harvester Fuel Consumption and Air Pollution Reduction. *Water Air Soil Pollut* **2020**, *231*, 95, doi:10.1007/s11270-020-4466-5.

62. Doungpueng, K.; Chuan-Udom, S.; Numsong, A.; Chansrakoo, W. Lost Times of Harvesting Processes of the Thai Combine Harvesters. *IOP Conf. Ser.: Earth Environ. Sci.* **2019**, *301*, 012018, doi:10.1088/1755-1315/301/1/012018.
63. Bochtis, D.D.; Sørensen, C.G.C.; Busato, P. Advances in Agricultural Machinery Management: A Review. *Biosystems Engineering* **2014**, *126*, 69–81, doi:10.1016/j.biosystemseng.2014.07.012.
64. Olt, J.; Küüt, K.; Ilves, R.; Küüt, A. Assessment of the Harvesting Costs of Different Combine Harvester Fleets. *Res. Agr. Eng.* **2019**, *65*, 25–32, doi:10.17221/98/2017-RAE.
65. 6° Censimento generale dell'agricoltura: dati provvisori Available online: https://www.istat.it/it/archivio/32618 (accessed on 26 January 2023).
66. Latterini, F.; Stefanoni, W.; Sebastiano, S.; Baldi, G.M.; Pari, L. Evaluating the Suitability of a Combine Harvester Equipped with the Sunflower Header to Harvest Cardoon Seeds: A Case Study in Central Italy. *Agronomy* **2020**, *10*, 1981, doi:10.3390/agronomy10121981.